System Science approach to the Space Weather Forecast

M. Balikhin

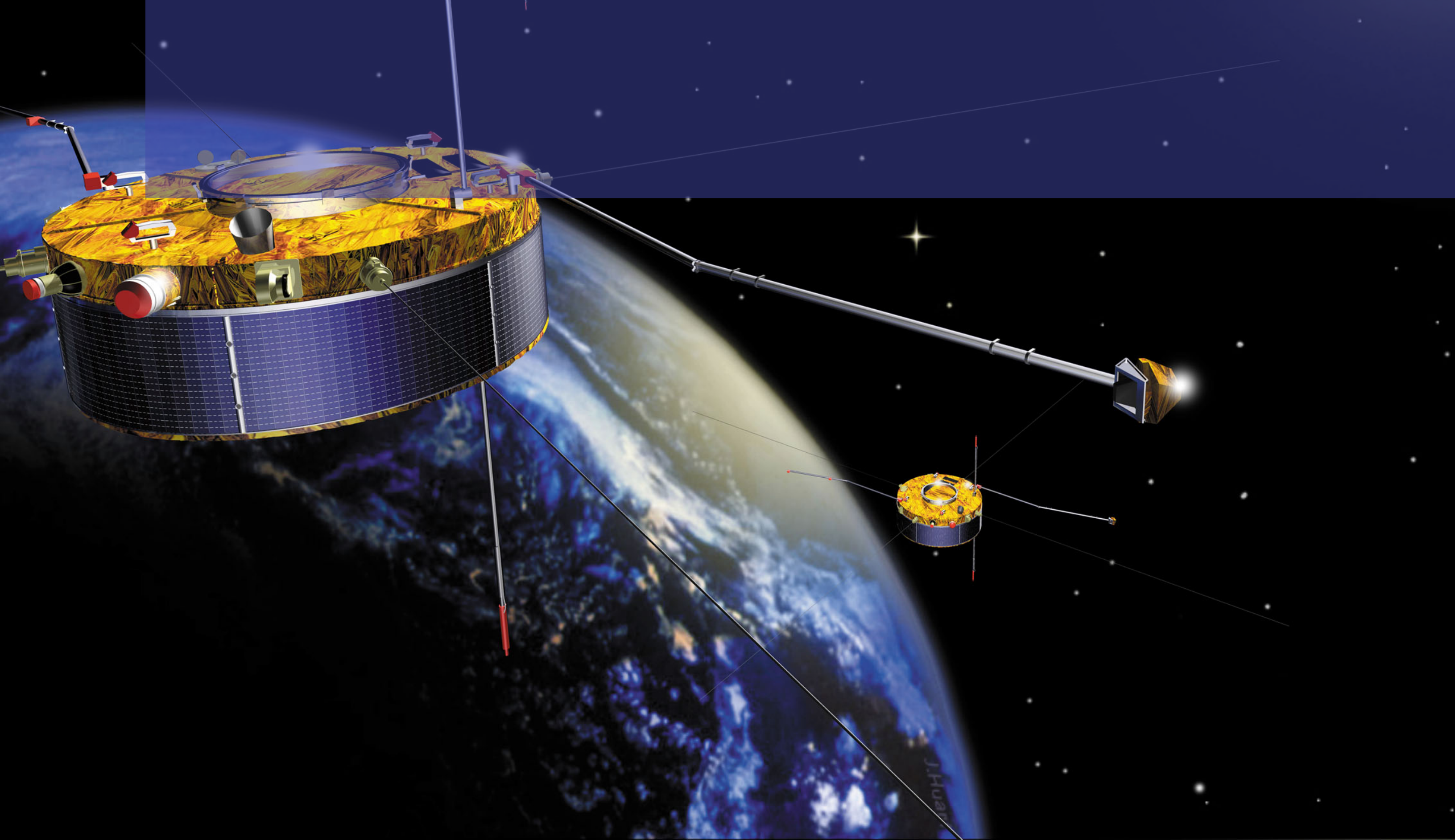

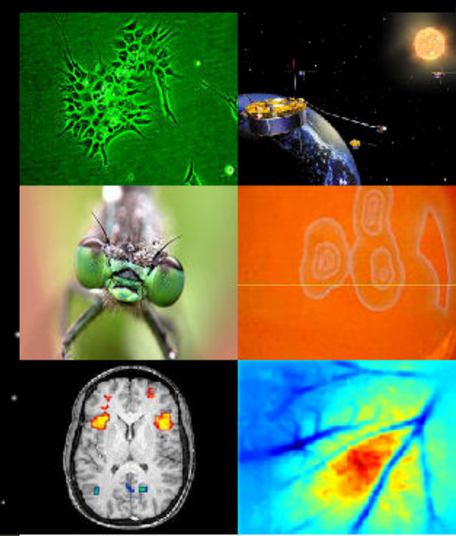

Participants

- University of Sheffield
- Finnish Meteorological Institute
- University of Warwick
- Skolkovo Institute of Science and Technology
- University of Michigan
- Space Research Institute, Ukraine
- LPC2E, France
- Swedish Institute for Space Physics

Collaborators

- Berkeley University
- UCLA

PROGRESS has received funding from the *European Union's Horizon 2020* under grant agreement No 637302.

PROGRESS

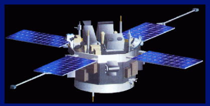

Geomagnetic indices Forecast

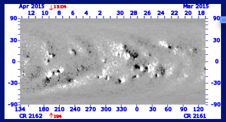

AWSoM → SWIFT

NARMAX

Solar Wind Parameters Forecast

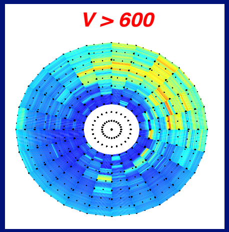

ERR

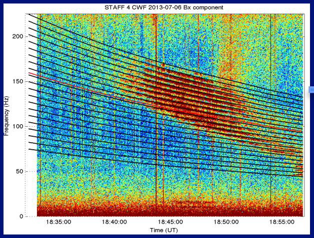

Cluster IMG

VERB

IMPTAM

NB^{3}GEO

Forecast of Radiation Environment in Geospace

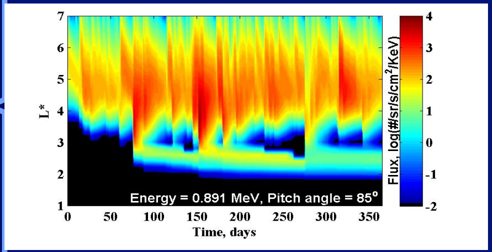

“Physics” based versus data based forecas

First Principles based forecast

$$S = \int L(x, \dot{x}, t)\, dt$$

$$dL = \sum_i \frac{\partial L}{\partial x_i} dx_i + \sum_i \frac{\partial L}{\partial \dot{x}_i} d\dot{x}_i$$

Assumptions

+

Physical Knowledge

+

First Principles

“Physics” based versus data based forecast

First Principles based forecast

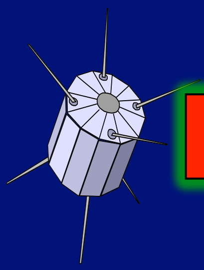

$$S = \int L(x, \dot{x}, t)\,dt$$

$$dL = \sum_i \frac{\partial L}{\partial x_i} dx_i + \sum_i \frac{\partial L}{\partial \dot{x}_i} d\dot{x}_i$$

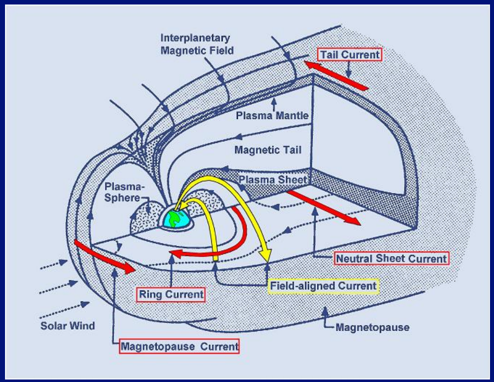

L1

Forecast

“Physics” based versus data based forecast

First Principles based forecast of high energy fluxes of Radiation belts

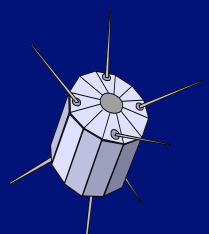

L1

Forecast

"Physics" based versus data based forecast

First Principles based forecast of high energy fluxes of Radiation belts

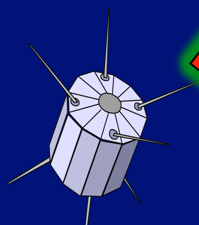

L1

$$S = \int L(x, \dot{x}, t)\,dt$$

$$dL = \sum_i \frac{\partial L}{\partial x_i} dx_i + \sum_i \frac{\partial L}{\partial \dot{x}_i} d\dot{x}_i$$

Boundary conditions

Forecast

“Physics” based versus data based forecast

First Principles based forecast of high energy fluxes of Radiation belts

$$S=\int L(x,\dot{x},t)\,dt$$

$$dL=\sum_i \frac{\partial L}{\partial x_i}dx_i+\sum_i \frac{\partial L}{\partial \dot{x}_i}d\dot{x}_i$$

Boundary conditions

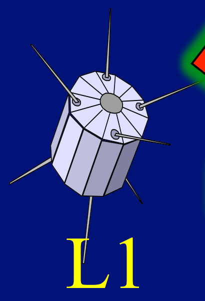

$$S=\int L(x,\dot{x},t)\,dt$$

$$dL=\sum_i \frac{\partial L}{\partial x_i}dx_i+\sum_i \frac{\partial L}{\partial \dot{x}_i}d\dot{x}_i$$

Model of the magnetic field

Forecast

“Physics” based versus data based forecast

First Principles based forecast of high energy fluxes of Radiation belts

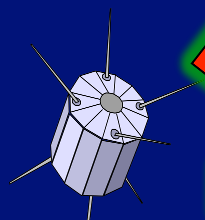

L1

$$S=\int L(x,\dot{x},t)\,dt$$

$$dL=\sum_i \frac{\partial L}{\partial x_i}dx_i+\sum_i \frac{\partial L}{\partial \dot{x}_i}d\dot{x}_i$$

Boundary conditions

$$S=\int L(x,\dot{x},t)\,dt$$

$$dL=\sum_i \frac{\partial L}{\partial x_i}dx_i+\sum_i \frac{\partial L}{\partial \dot{x}_i}d\dot{x}_i$$

Model of the magnetic field

$$S=\int L(x,\dot{x},t)\,dt$$

$$dL=\sum_i \frac{\partial L}{\partial x_i}dx_i+\sum_i \frac{\partial L}{\partial \dot{x}_i}d\dot{x}_i$$

Wave model for the distribution of Hiss, Chorus, EMW, EMIC

Forecast

"Physics" based versus data based forecast

First Principles based forecast of high energy fluxes of Radiation belts

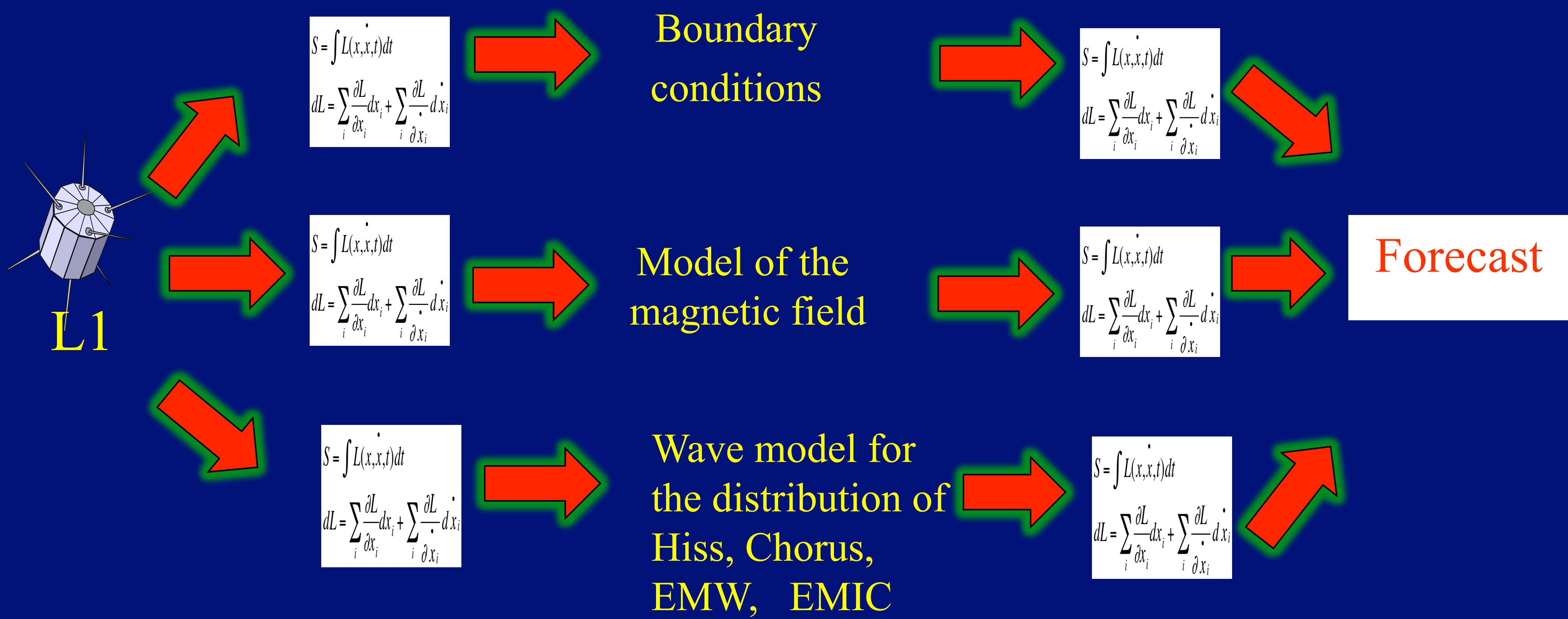

“Physics” based versus data based forecast

First Principles based forecast of high energy fluxes of Radiation belts

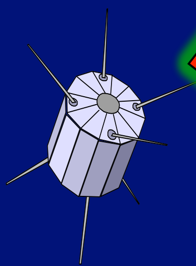

$$S=\int L(x,\dot{x},t)\,dt$$

$$dL=\sum_i \frac{\partial L}{\partial x_i}dx_i+\sum_i \frac{\partial L}{\partial \dot{x}_i}d\dot{x}_i$$

Boundary conditions

Forecast

“Physics” based versus data based forecast

First Principles based forecast of high energy fluxes of Radiation belts

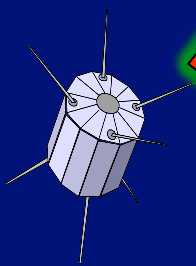

Tsyganenko
Mukai 2003

Boundary
conditions

Forecast

“Physics” based versus data based forecast

First Principles based forecast of high energy fluxes of Radiation belts

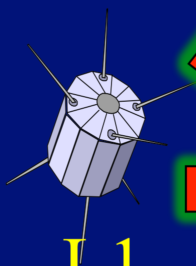

L1

Tsyganenko Mukai 2003 → Boundary conditions

Tsyganenko model → Model of the magnetic field

Forecast

“Physics” based versus data based forecast

First Principles based forecast of high energy fluxes of Radiation belts

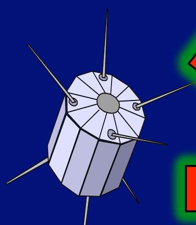

L1

Tsyganenko Mukai 2003 → Boundary conditions

Tsyganenko → Model of the magnetic field

Empirical wave models → Wave model

Kp, AE

Forecast

“Physics” based versus data based forecast

First Principles based forecast of high energy fluxes of Radiation belts

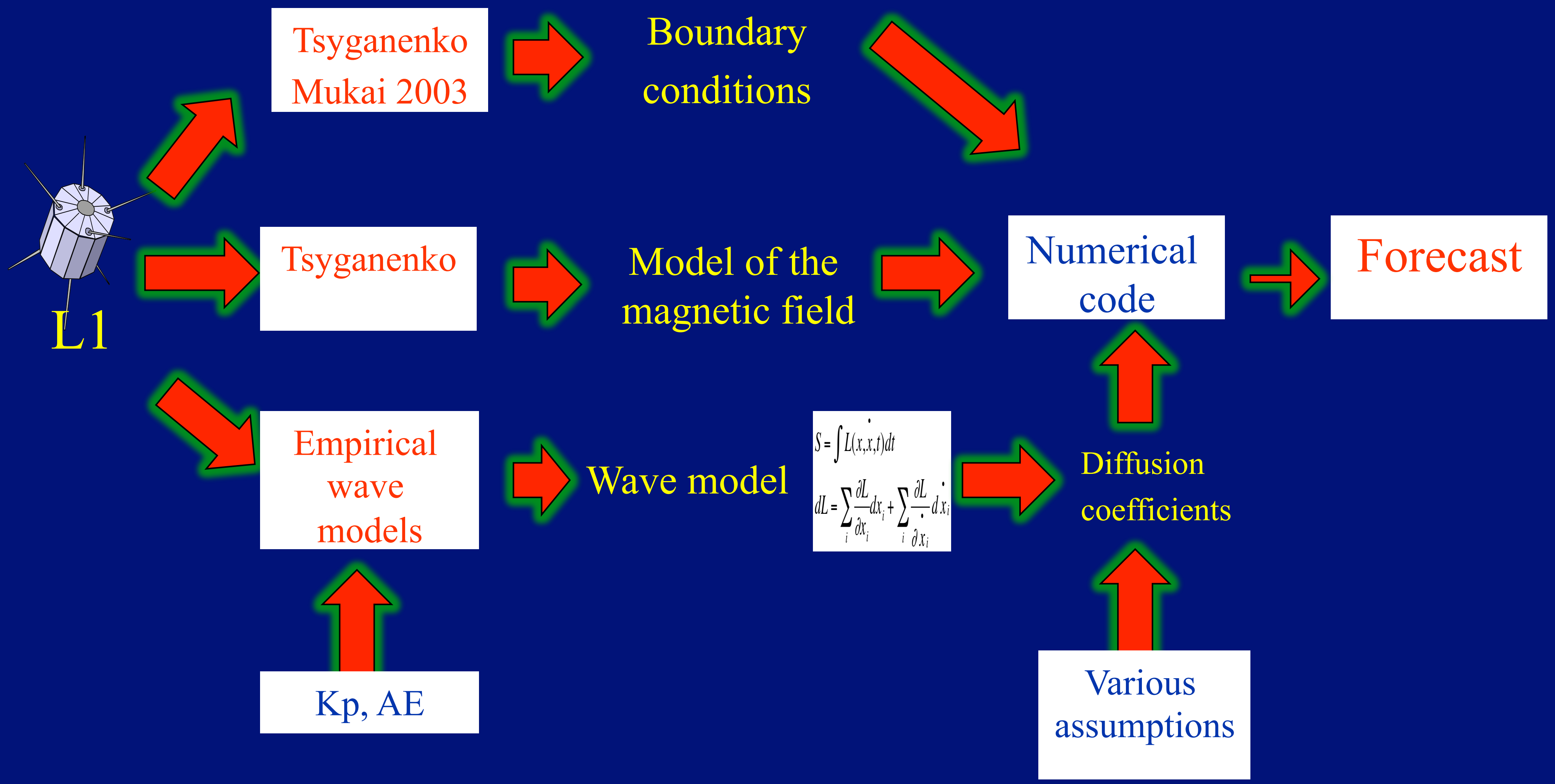

“Physics” based versus data based forecast

First Principles based forecast of high energy fluxes of Radiation belts

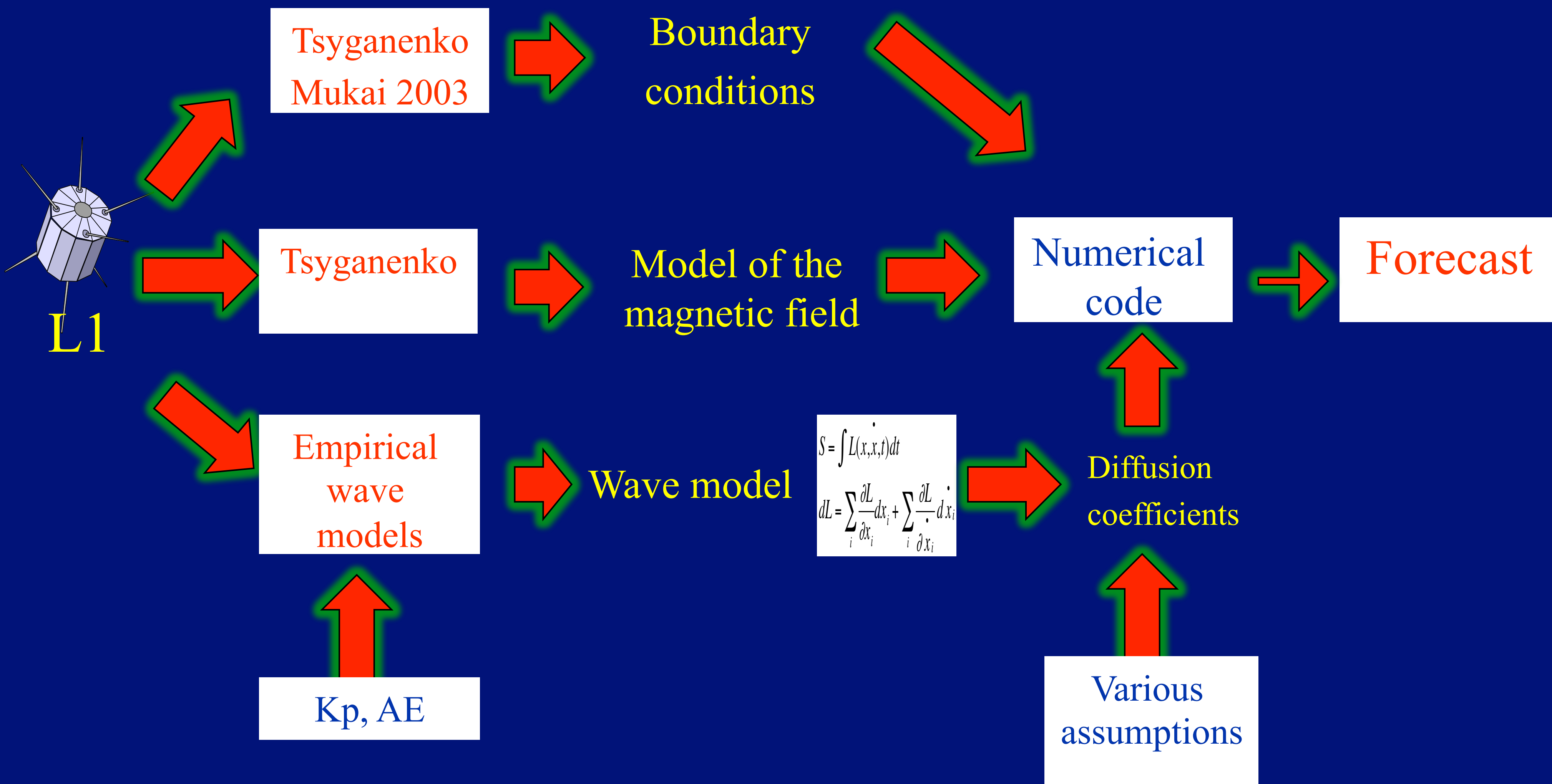

“Physics” based versus data based forecast

First Principles based forecast of high energy fluxes of Radiation belts

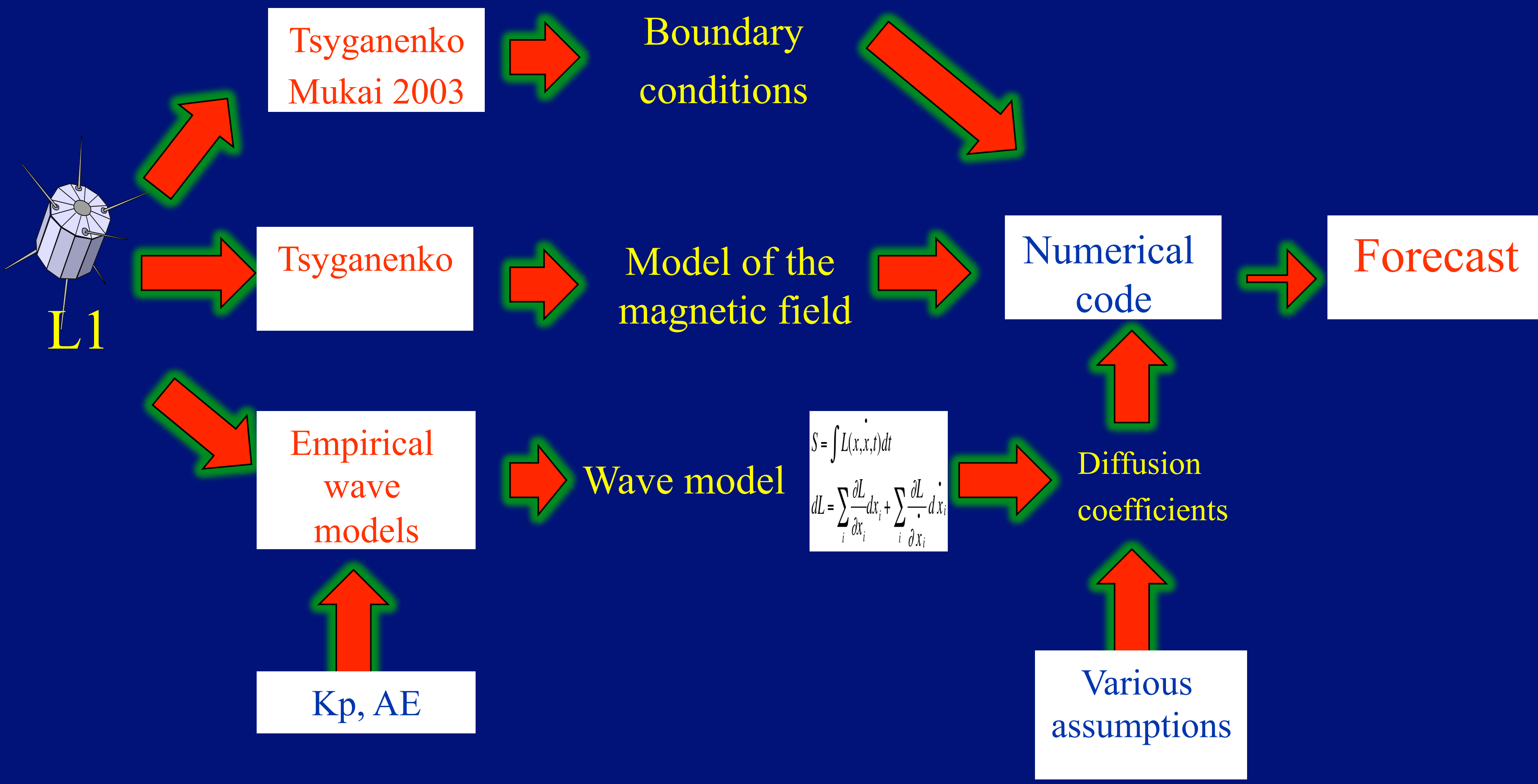

“Physics” based versus data based forecast

First Principles based forecast of high energy fluxes of Radiation belts

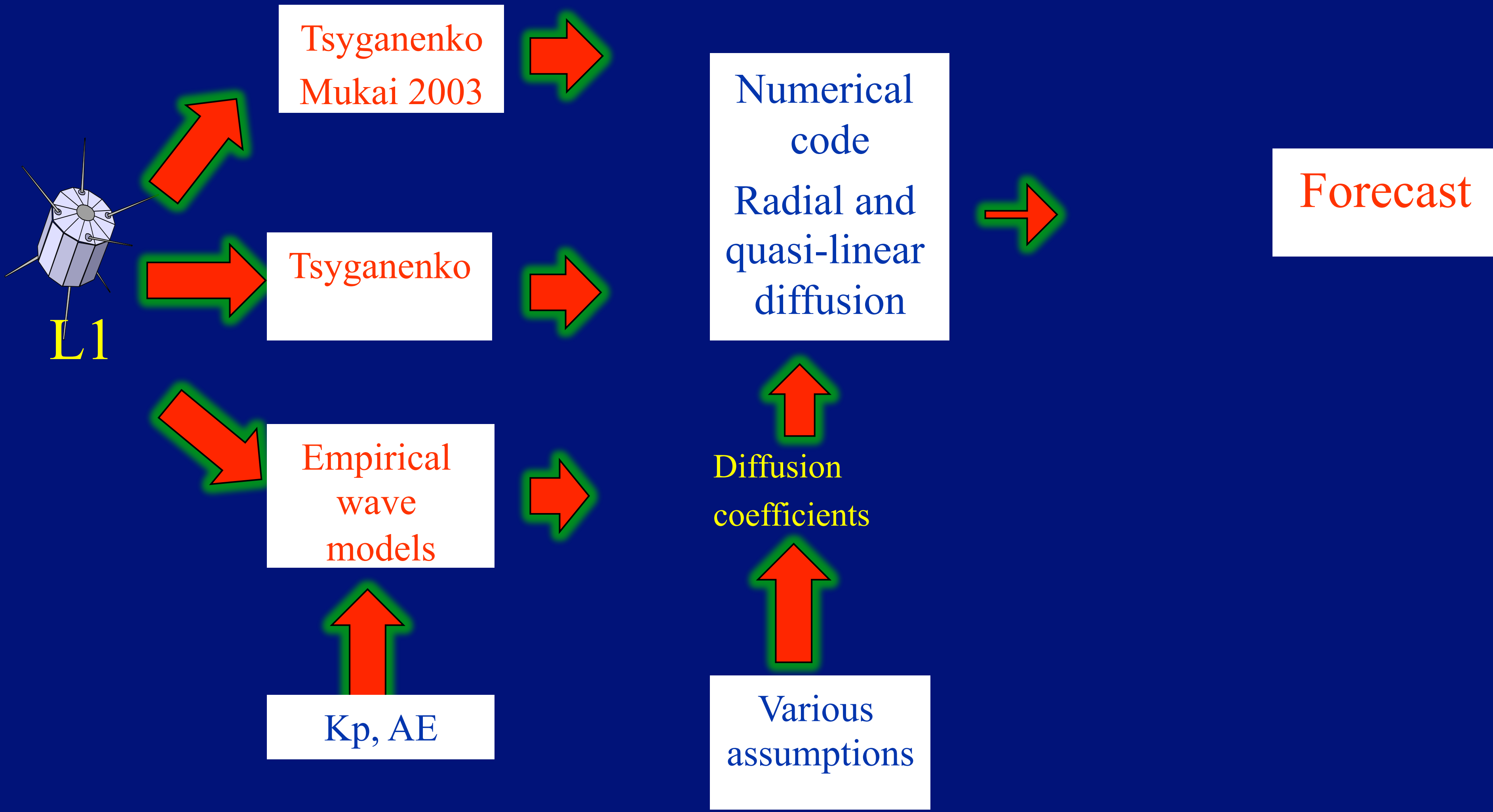

“Physics” based versus data based forecast

First Principles based forecast of high energy fluxes of Radiation belts

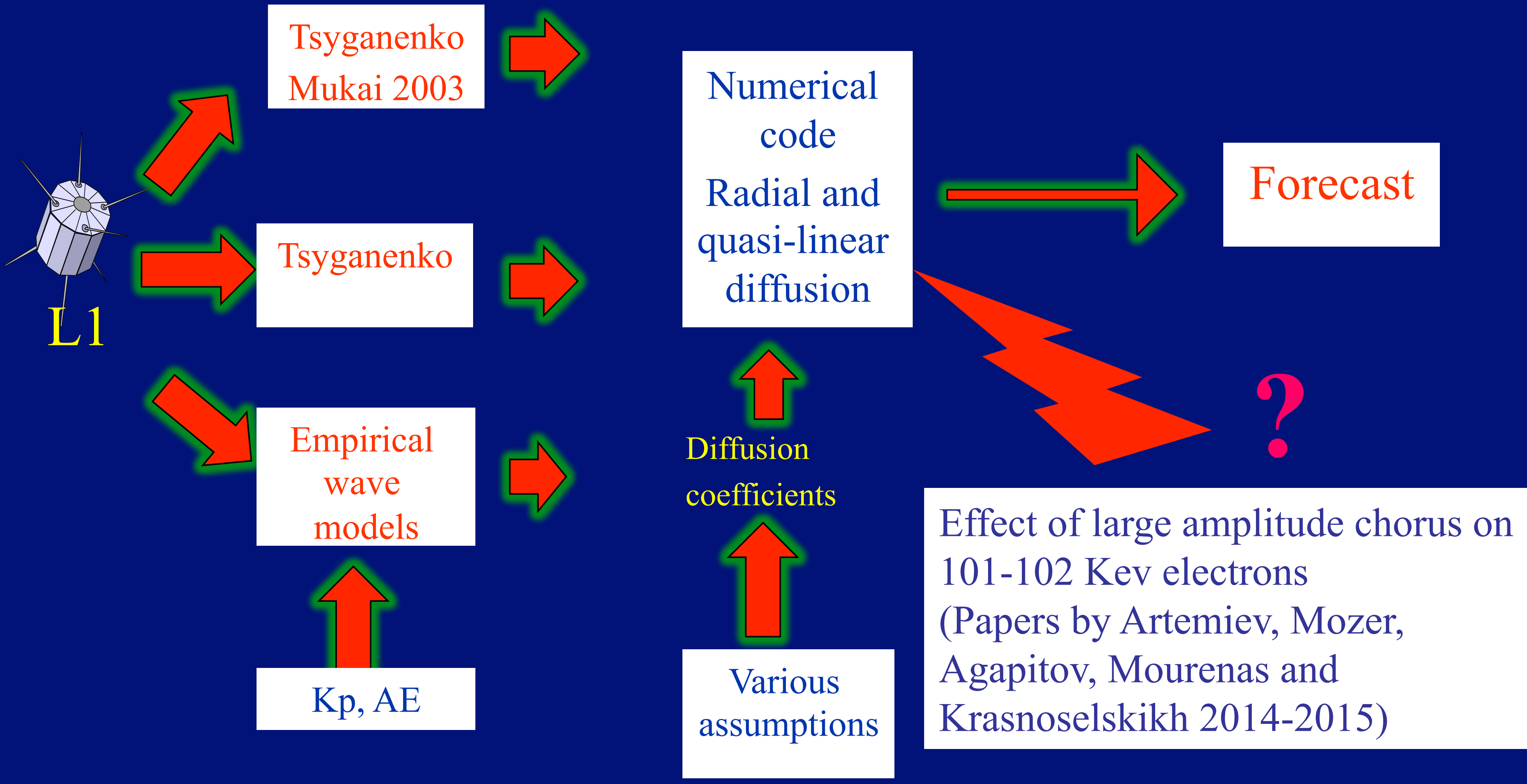

"Physics" based versus data based forecast

First Principles based forecast of high energy fluxes of Radiation belts

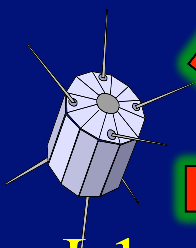

L1

Tsyganenko Mukai 2003

Tsyganenko

Empirical wave models

Kp, AE

Numerical code

Radial and quasi-linear diffusion

Diffusion coefficients

Various assumptions

Forecast

Whenever a theory appears to you as the only possible one, take this as a sign that you have neither understood the theory nor the problem which it was intended to solve.

Karl Raimund Popper

System Identification Approach

Analytical Approach

$$S = \int L(x, \dot{x}, t)\,dt$$

$$dL = \sum_i \frac{\partial L}{\partial x_i} dx_i + \sum_i \frac{\partial L}{\partial \dot{x}_i} d\dot{x}_i$$

Assumptions

+

Physical Knowledge

+

First Principles

Black box System

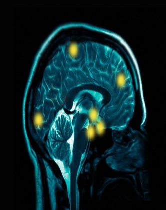

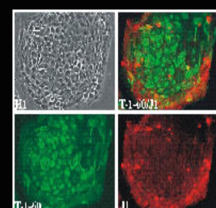

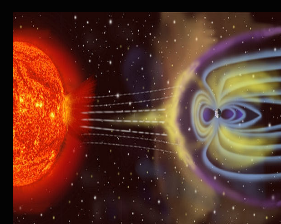

Systems Approach

Knowledge of the System

$$S = \int L(x, \dot{x}, t)\,dt$$

$$dL = \sum_i \frac{\partial L}{\partial x_i} dx_i + \sum_i \frac{\partial L}{\partial \dot{x}_i} d\dot{x}_i$$

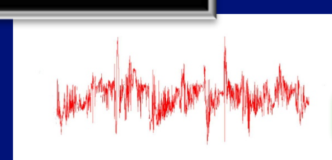

Input Data

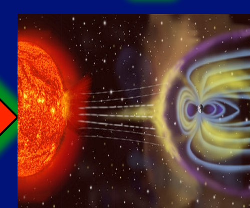

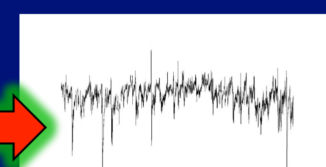

Output Data

Systems Science tools for nonlinear systems

Neural Nets

NARMAX

Genetic Algorithms

SVM

Fuzzy Logic

Frequency domain methods

The NARMAX approach

- the NARMAX model is given as:

$$y(k) = F[y(k-1),\ldots y(k-n_y),u(k),\ldots,u(k-n_u),\xi(k-1),\ldots,\xi(k-n_\xi)] + \xi(k)$$

$y(k)$: system output

$u(k)$: system input

$\xi(k)$: noise

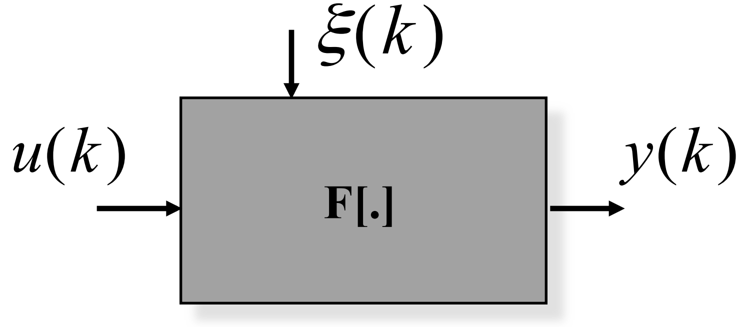

$F[\cdot]$ nonlinear function (polynomial, rational, B-spline, RBF)

The NARMAX approach

Identification methodology:

- Structure detection: Orthogonal Least-Squares estimator (ERR structure detection)
- Parameter estimation
- Model validation:
  - statistical validation
  - dynamical validation

$$\frac{dy}{dt} = 3.1\frac{dx}{dt} + 4.2x - \frac{xdx}{dt} + 2x^3$$

Model Structure: $x; x^3; \frac{dx}{dt}; \frac{xdx}{dt}.$

Dst

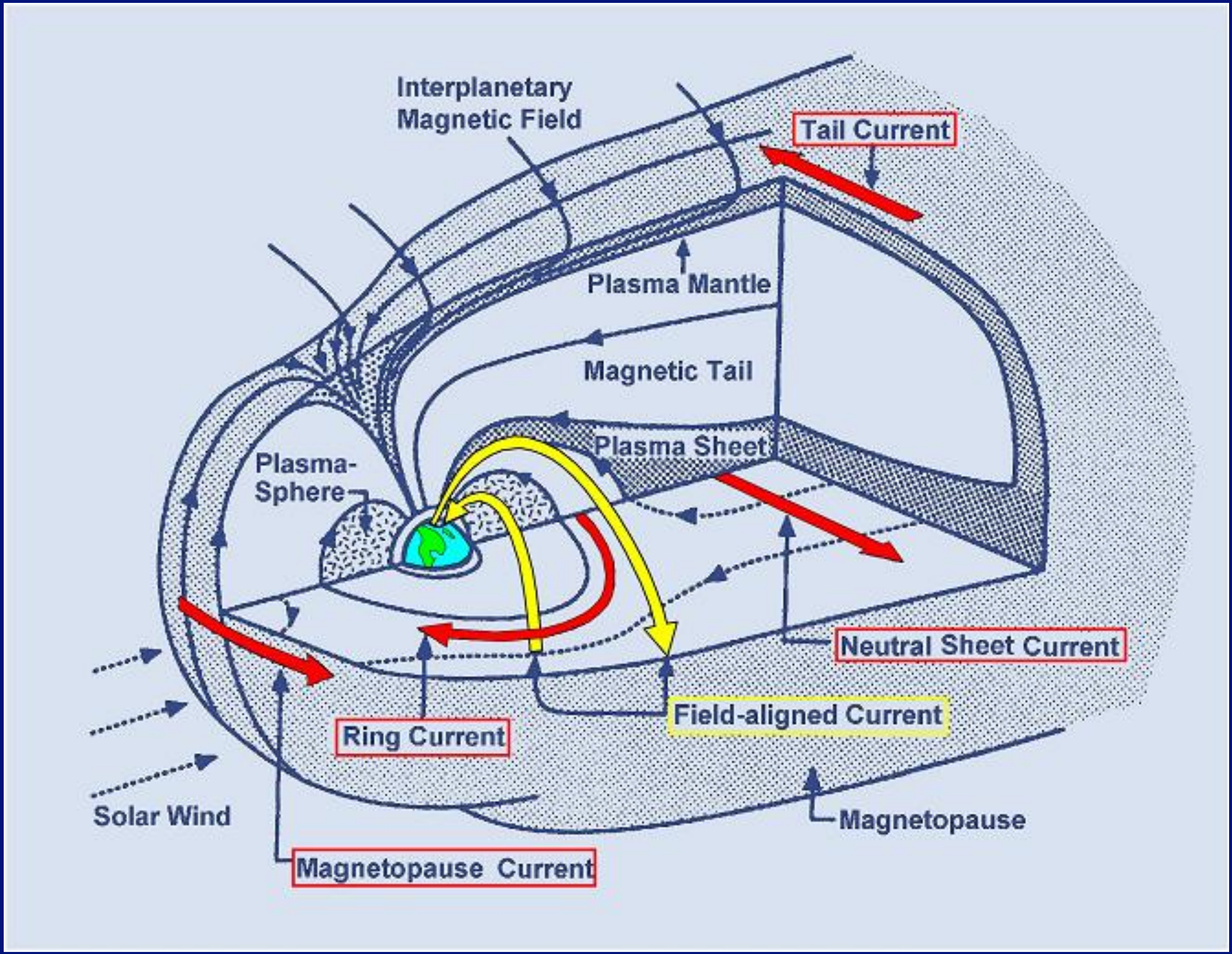

Interplanetary Magnetic Field
Tail Current
Plasma Mantle
Magnetic Tail
Plasma Sheet
Plasma-Sphere
Neutral Sheet Current
Field-aligned Current
Ring Current
Solar Wind
Magnetopause
Magnetopause Current

Analytical approach to coupling functions

1. Burton et al 1975 VBs
2. Perreault and Akasofu [1974] $\varepsilon = VB^2 \sin(\theta/2)^4 l_0^2$,
3. Kan and Lee 1979

Analytical approach to coupling functions

4. $V^{4/3}B_T\sin^2(\theta/2)P^{1/6}$, $V^{4/3}B_T\sin^4(\theta/2)P^{1/6}$ [Vasyliunas et al., 1982],

5. $VB_T\sin^4(\theta/2)P^{1/2}$ [Scurry and Russell,1991],

6. $n^{1/2}V^2B_T\sin^6(\theta/2)$ [Temerin and Li, ,2006],

7. $V^{4/3}B^{2/3}{}_T\sin^{8/3}(\theta/2)$ [Newell et al., 2007],

8. $VB_T\sin^4(\theta/2)$ [Wygant et al., 1983] and its modifications $[VB_T\sin^4(\theta/2)]^2$, $[VB_T\sin^4(\theta/2)]^{1/2}$.

Solar Wind Magnetosphere "Coupling Functions"

Name	Functional Form	Reference
B_z	B_z	*Dungey* [1961]
Velocity	v	*Crooker et al.* [1977]
Density	n	
p	$nv^2/2$	*Chapman and Ferraro* [1931]
Bs	B_z ($B_z < 0$); 0 ($B_z > 0$)	
Half-wave rectifier	vBs	*Burton et al.* [1975]
ε	$vB^2\sin^4(\theta_c/2)$	*Perrault and Akasofu* [1978]
ε_2	$vB_T^2\sin^4(\theta_c/2)$	Variant on ε
ε_3	$vB\sin^4(\theta_c/2)$	Variant on ε
Solar wind E-field	vB_T	
E_{KL}	$vB_T\sin^2(\theta_c/2)$	*Kan and Lee* [1979]
$E_{KL}^{1/2}$	$[\mathrm{v}\mathrm{B}_\mathrm{T}\sin^2(\theta_c/2)]^{1/2}$	Variant on the Kan-Lee electric field
E_{KLV}	$v^{4/3}B_T\sin^2(\theta_c/2)\mathrm{p}^{1/6}$	*Vasyliunas et al.* [1982]
E_{WAV}	$vB_T\sin^4(\theta_c/2)$	*Wygant et al.* [1983]
E_{WAV}^2	$[vB_T\sin^4(\theta_c/2)]^2$	Variant on E_{WAV}
$E_{WAV}^{1/2}$	$[vB_T\sin^4(\theta_c/2)]^{1/2}$	Variant on E_{WAV}
E_{WV}	$v^{4/3}B_T\sin^4(\theta_c/2)p^{1/6}$	*Vasyliunas et al.* [1982]
E_{SR}	$vB_T\sin^4(\theta_c/2)p^{1/2}$	*Scurry and Russell* [1991]
E_{TL}	$n^{1/2}v^2B_T\sin^6(\theta_c/2)$	*Temerin and Li* [2006]
$d\Phi_{MP}/dt$	$v^{4/3}B_T^{2/3}\sin^{8/3}(\theta_c/2)$	This paper

From Newell et al., 2007

Data based approach

Correlation function usually is a primary tool (e.g. Newell et al., 2007)

Table 2. Various Possible Viscous Solar Wind Coupling Functions, Ranked According to Their Ability to Predict Variance in 10 Magnetospheric State Variables

Rank, f	Λ_c	Dst	AE	AU	Goes	Kp	Auro	b2i	Φ_{PC}	AL	$\Sigma r^2/n$
1. $n^{1/2}v^2$	−0.364	−0.500	0.469	0.430	−0.325	0.670	0.510	−0.520	0.319	−0.225	22.3%
2. $n^{1/3}v^2$	−0.371	−0.497	0.458	0.389	−0.353	0.678	0.512	−0.460	0.324	−0.250	21.8%
3. $n^{1/2}v^3$	−0.363	−0.517	0.452	0.383	−0.340	0.653	0.515	−0.449	0.317	−0.236	21.1%
4. $n^{1/6}v^2$	−0.353	−0.460	0.416	0.330	−0.347	0.628	0.471	−0.382	0.294	−0.254	18.5%
5. nv^3	−0.331	−0.507	0.425	0.421	−0.260	0.549	0.488	−0.516	0.272	−0.153	18.5%
6. $nv^{5/2}$	−0.312	−0.457	0.383	0.401	−0.239	0.525	0.448	−0.511	0.249	−0.124	16.3%
7. $v^{4/3}$	−0.374	−0.408	0.372	0.277	−0.321	0.547	0.402	−0.314	0.252	−0.250	14.7%
8. v	−0.324	−0.406	0.374	0.279	−0.321	0.537	0.399	−0.315	0.254	−0.251	14.7%
9. $v^{3/2}$	−0.321	−0.408	0.372	0.276	−0.319	0.549	0.404	−0.312	0.251	−0.249	14.7%
10. v^2	−0.317	−0.409	0.369	0.272	−0.311	0.547	0.407	−0.310	0.247	−0.246	14.4%
11. $v^{2/3}$	−0.325	−0.405	0.374	0.281	−0.311	0.503	0.396	−0.316	0.255	−0.252	14.4%
12. $v^{1/2}$	−0.325	−0.403	0.374	0.282	−0.294	0.465	0.395	−0.316	0.255	−0.252	14.0%
13. p	−0.277	−0.373	0.316	0.357	−0.202	0.469	0.391	−0.474	0.217	−0.085	12.5%
14. $p^{2/3}$	−0.272	−0.321	0.326	0.365	−0.199	0.486	0.377	−0.485	0.228	−0.101	12.4%
15. $p^{1/2}$	−0.267	−0.295	0.329	0.367	−0.194	0.482	0.366	−0.486	0.231	−0.108	12.2%
16. $p^{1/3}$	−0.193	−0.269	0.331	0.366	−0.186	0.463	0.353	−0.485	0.231	−0.115	11.7%
17. $p^{3/2}$	−0.274	−0.427	0.288	0.331	−0.183	0.394	0.397	−0.431	0.190	−0.057	11.1%
18. p^2	−0.257	−0.420	0.250	0.292	−0.150	0.288	0.387	−0.351	0.159	−0.031	8.5%
19. nv	−0.163	−0.149	0.143	0.221	−0.089	0.287	0.253	−0.325	0.136	0.004	4.0%
20. n	−0.041	0.030	0.001	0.093	0.033	0.103	0.122	−0.172	0.058	0.070	0.6%

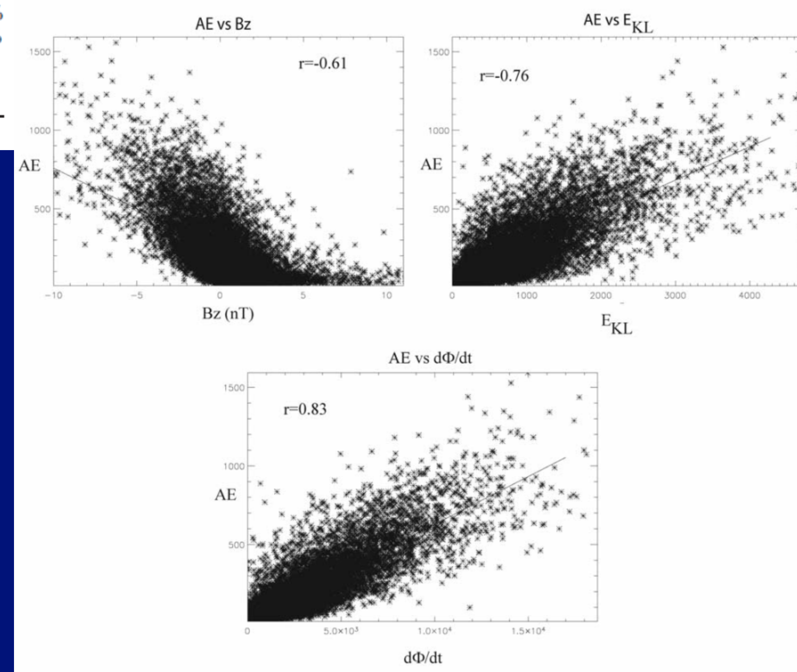

Solar Wind Magnetosphere "Coupling Functions"

X(t) → $y=x^2$ → Y(t)

5% Noise

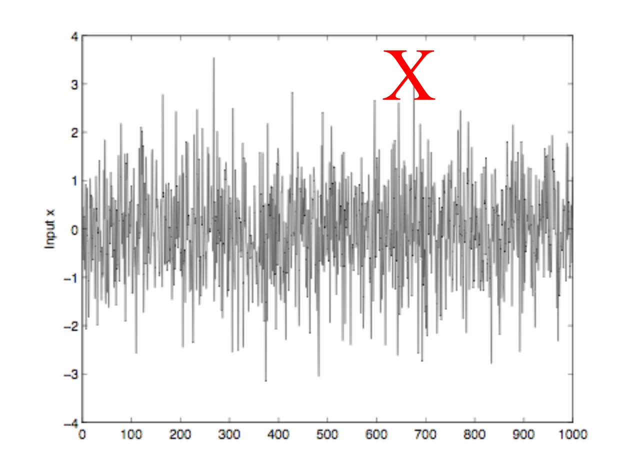

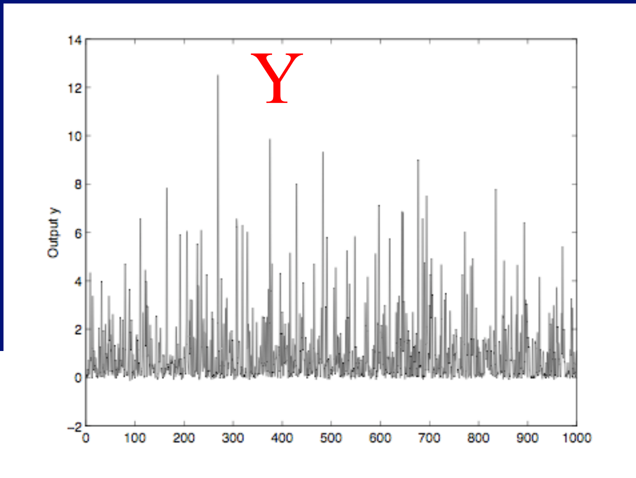

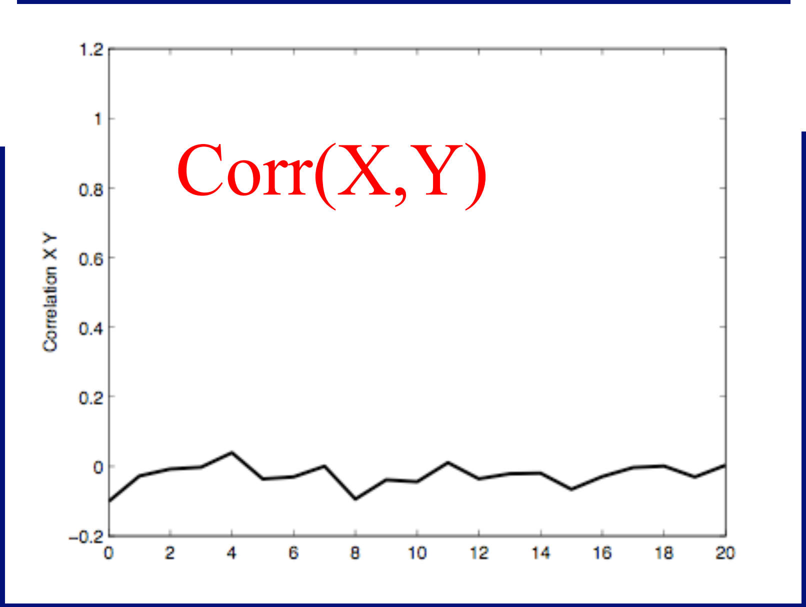

(X, Y)

(X^2, Y)

....

(X^k, Y)

(X^{k+1}, Y)

....

Previously proposed coupling functions

1. $I_B = VB_s$ by *Burton et al.* [1975]
2. $\varepsilon = VB^2 \sin^4(\theta/2)$, by *Perreault and Akasofu* [1978]
3. $I_W = VB_T \sin^4(\theta/2)$ by *Wygant et al.* [1983]
4. $I_{SR} = p^{1/2} VB_T \sin^4(\theta/2)$ by *Scurry and Russell* [1991]
5. $I_{TL} = p^{1/2} VB_T \sin^6(\theta/2)$ by *Temerin and Li* [2006]
6. $I_N = V^{4/3} B_T^{2/3} \sin^{8/3}(\theta/2)$ by *Newell et al.* [2007]
7. $I_V = n^{1/6} V^{4/3} B_T \sin^4(\theta/2)$ by *Vasyliunas et al.* [1982]

Coupling Function	NERR
$p^{1/2} VB_T \sin^6(\theta/2)(t\text{-}1)$	31.32
$VB_s(t\text{-}1)$	12.76
$n^{1/6} V^{4/3} B_T \sin^4(\theta/2)(t\text{-}1)$	10.30
$p^{1/2} VB_T \sin^4(\theta/2)(t\text{-}1)$	8.37
$D_{st}(t\text{-}2)$	7.23

$p^{1/2}V^2B_T\sin^6(\theta/2)$	**14.0**
$p^{1/2}V^{4/3}B_T\sin^6(\theta/2)$	**12.5**
$P^{1/2}VB_T\sin^6(\theta/2)$	**12.1**
VB_s	**8.91**

$\sin^6(\theta/2)$ or $\sin^4(\theta/2)$?

Where $\sin^4(\theta/2)$ did appear from?

Kan and Lee (1978) model

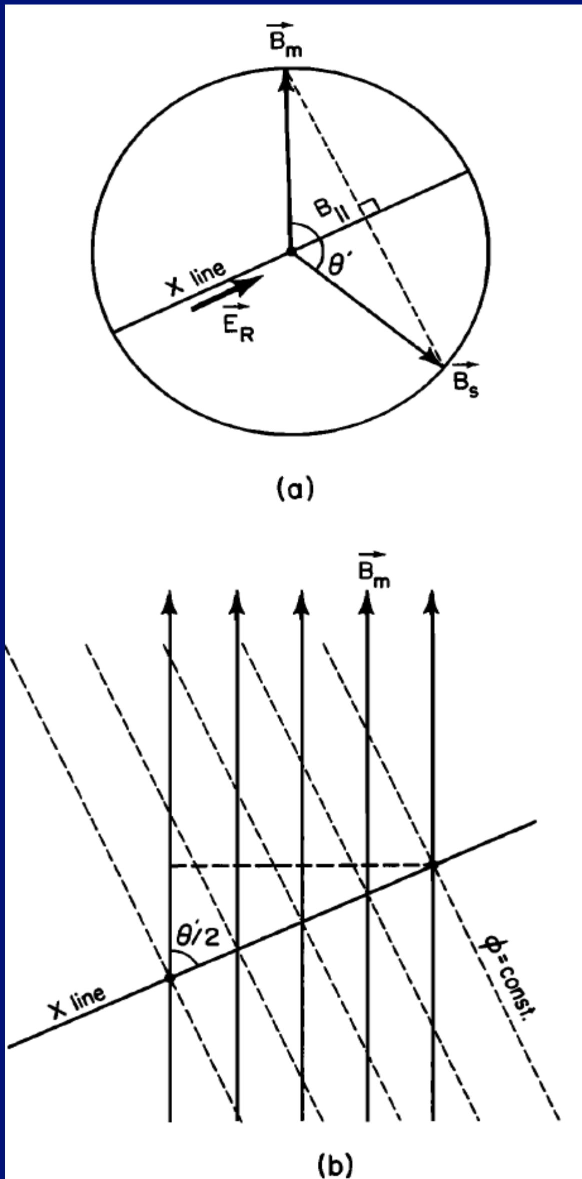

ig. 1. A schematic illustration of the field

$$E_R = V_s B_s \sin\left(\frac{\theta}{2}\right)$$

Reconnection Electric field for two magnetic fields of equal magnitudes: Sonnerup (1974) Russell and Atkinson (1973)

Kan and Lee stated that only perpendicular component of the electric field contributes to the potential across the polar

$$\Phi = \int E_{R\perp} dl_\perp = \int V_s B_s \sin^2\left(\frac{\theta}{2}\right) dl \sin\left(\frac{\theta}{2}\right)$$

$$\Phi = V_s B_s \sin^3\left(\frac{\theta}{2}\right) l_0$$

Finaly Kan and Lee argued that power delivered by solar wind dynamo is proportional to potential square divided effective system resistance:

$$P = \frac{\Phi^2}{R} = V_s^2 B_s^2 \sin^6\left(\frac{\theta}{2}\right) l_0^2$$

ENERGY COUPLING FUNCTION AND SOLAR WIND–MAGNETOSPHERE DYNAMO

J.R. Kan and L.C. Lee

The potential difference Φ_m across the polar cap is due to the perpendicular component of the reconnection electric field, i.e., $E_R \sin\theta/2$ as shown in Figure 1(b). This geometrical factor has been overlooked in the previous studies of component reconnection. Thus the polar cap potential Φ_m can be written as

$$\Phi_m = V_s B_s \sin^2(\theta/2)\, \ell_o \tag{3}$$

where ℓ_o is the effective length of the X line.

The power delivered by the solar wind dynamo is given by

$$P = \phi_m^2/R = V^2 B^2 \sin^4(\theta/2)\, \ell_o{}^2/R$$

$$= (V/R)\ \varepsilon(t) \tag{5}$$

Forecasting D_{st}

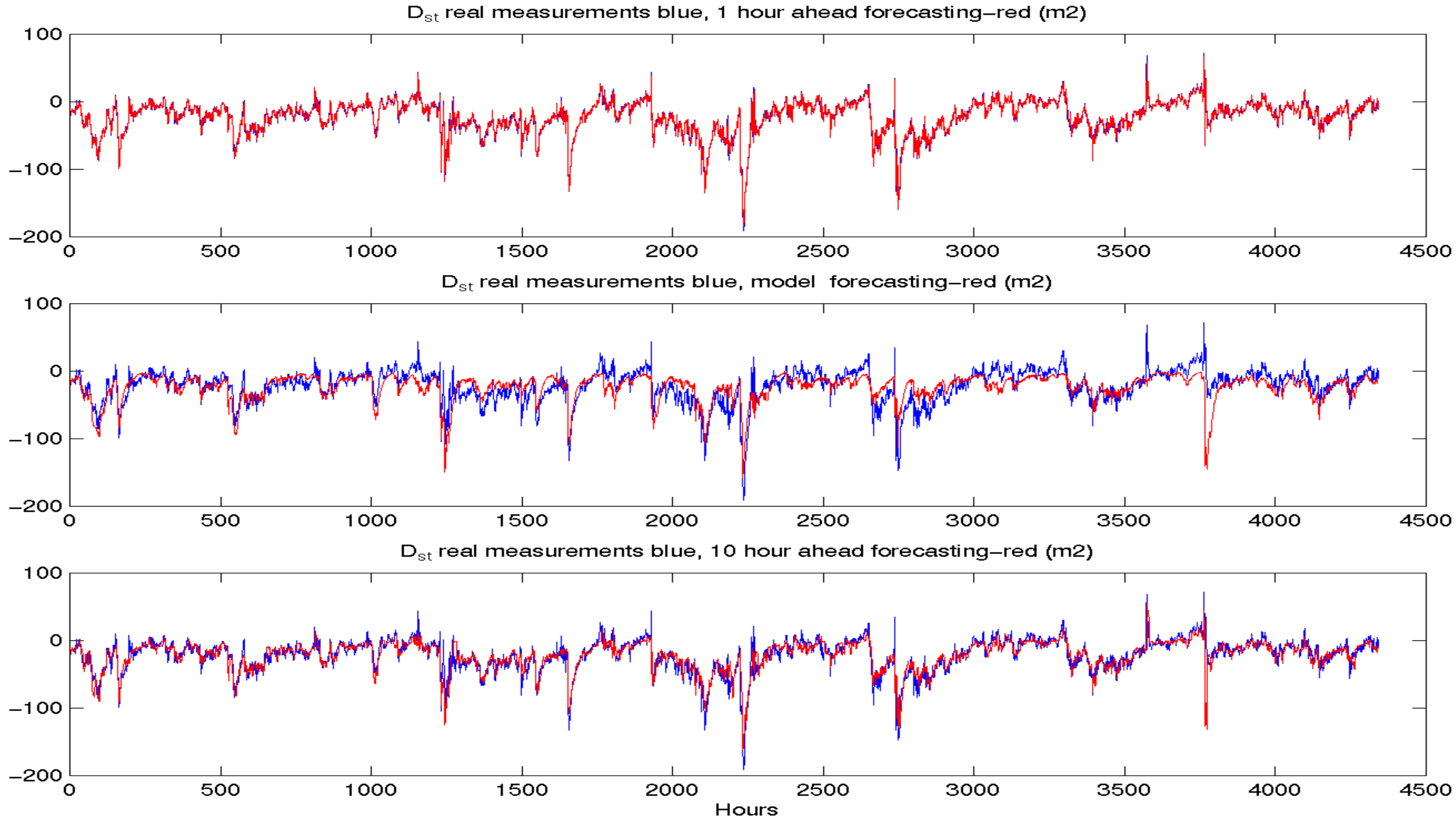

Earth's Radiation Belts

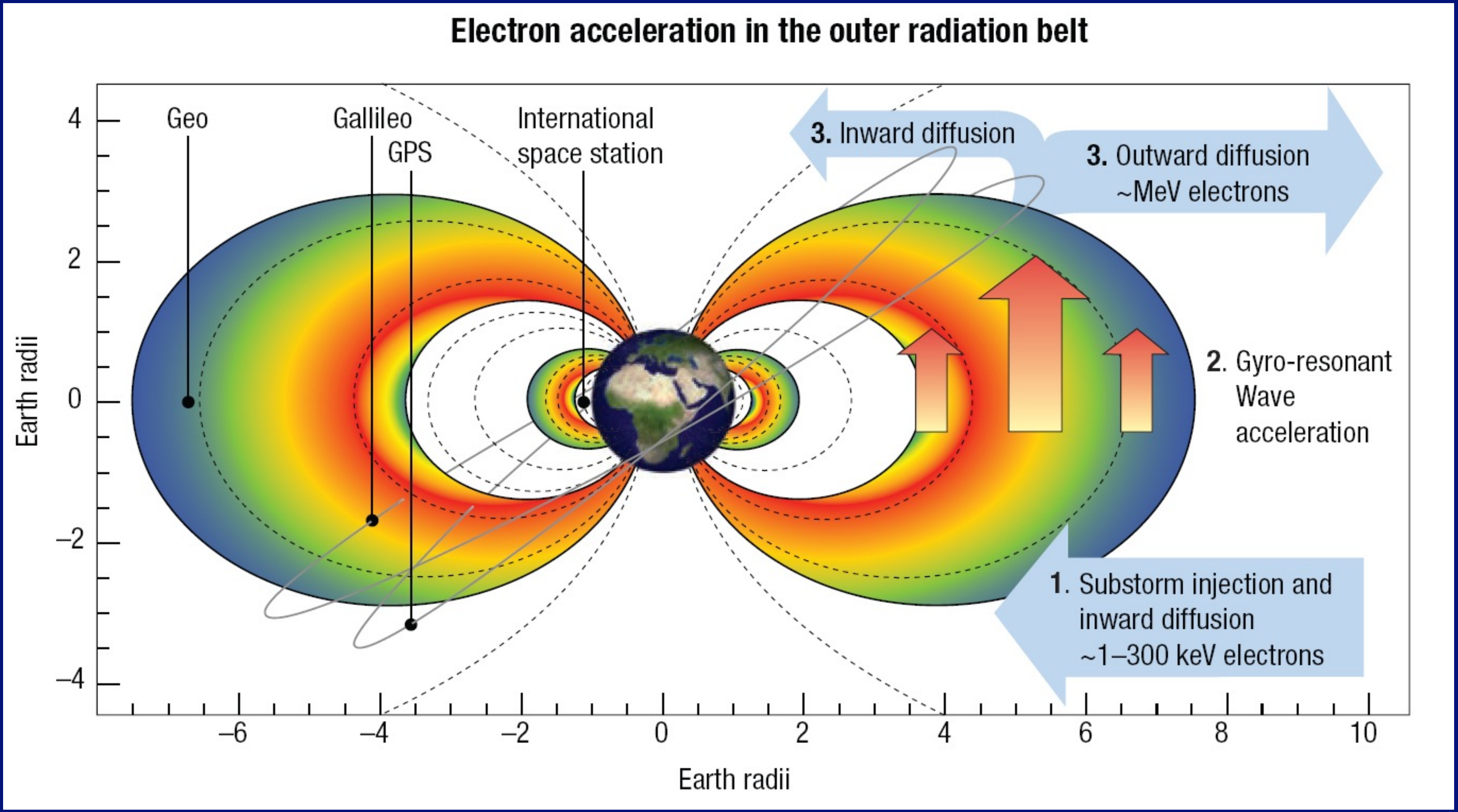

Numerical models for the forecast of radiation belts: Data Analysis

Paulikas, G. A., and J. B. Blake (1979),
Reeves et al., 2011 1.8-3.5MeV GEO

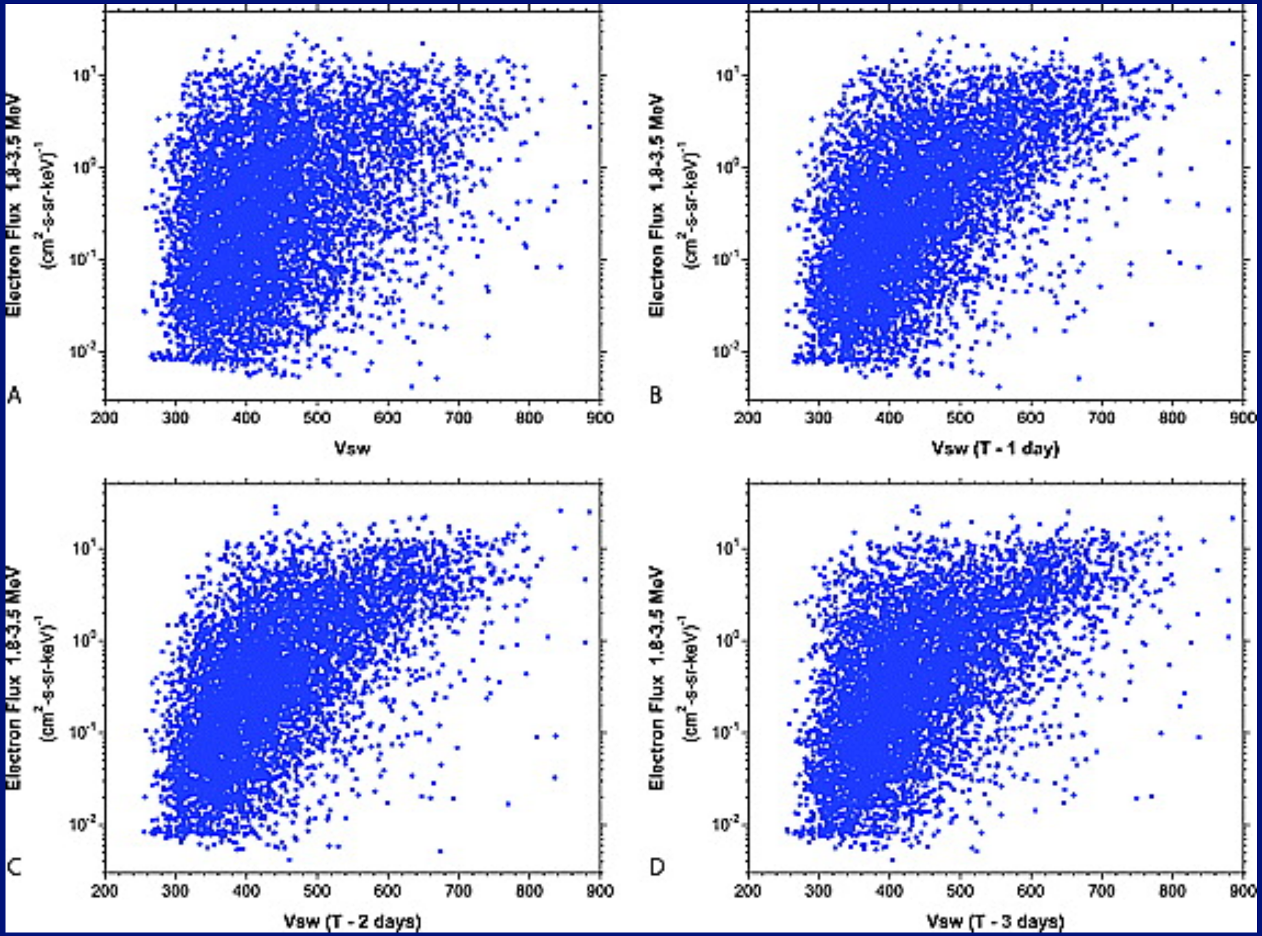

1.8-3.5 MeV: Solar wind parameters

2nd order nonlinearity

V, n, p, B_x, B_y, B_z

Parameter	NERR
$n(t\text{-}1)$	62.9
$n^2(t\text{-}1)$	15.0
$V^2(t\text{-}2)$	6.3
$V^2(t\text{-}4)$	4.6
$PV(t\text{-}1)$	2.2
$P^2(t\text{-}1)$	1.9
$V^2(t\text{-}1)$	1.0
$nB_z(t\text{-}2)$	0.83

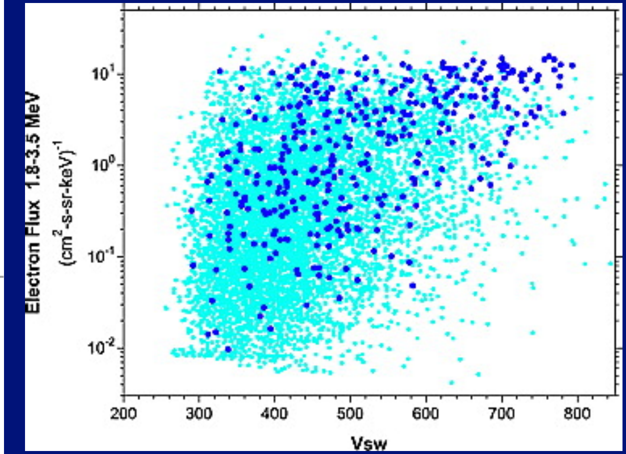

$cm^{-2}s^{-1}sr^{-1}KeV^{-1}$

Illustration by scatter plots.

Balikhin et al., 2011

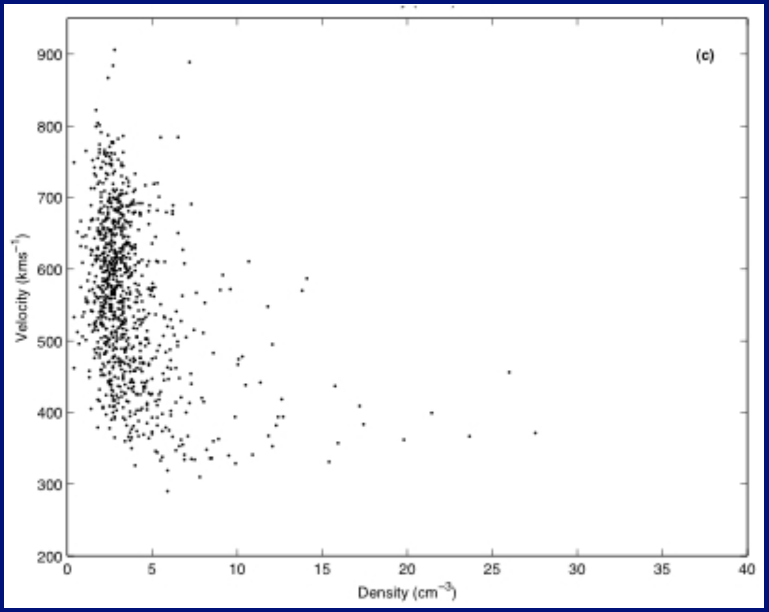

$$Log(Flux\ [cm^{-2}s^{-1}sr^{-1}KeV^{-1}]) > 0.5$$

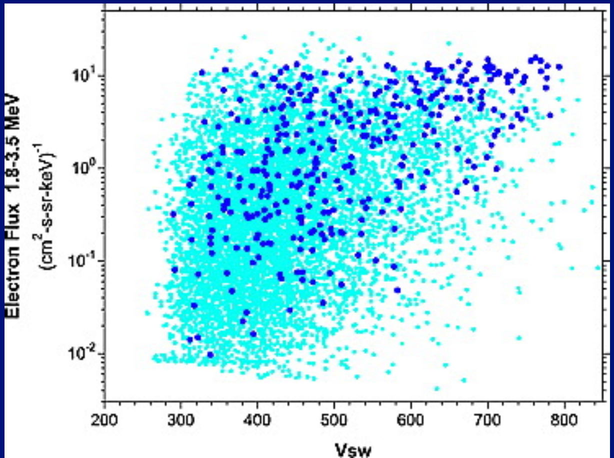

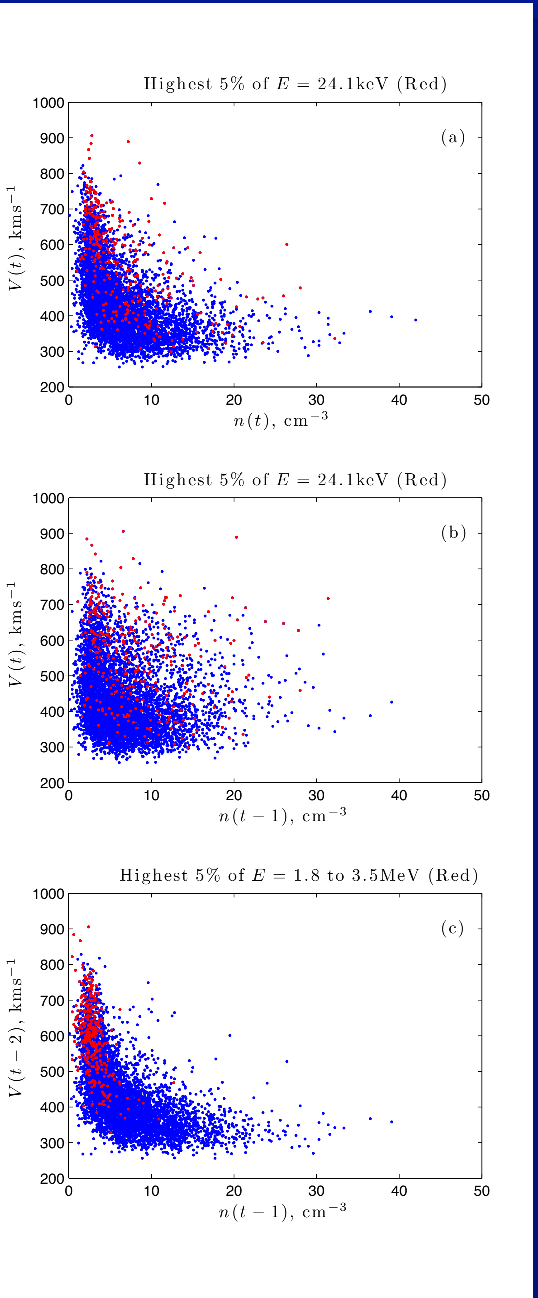

$$[\mathbf{k}\cdot(\mathbf{V_1}-\mathbf{V_2})] > \frac{n_1+n_2}{4\pi m_0 n_1 n_2}[(\mathbf{k}\cdot\mathbf{B_1})^2+(\mathbf{k}\cdot\mathbf{B_2})^2],$$

[*Mikhailovskii and Klimenko*, 1980]:

$$\gamma = \frac{k_\parallel V_A}{2}\left[\left(\frac{V^2}{V_A^2}\right)-4\right]^{\frac{1}{2}}$$

$$\left(\frac{n_i}{n_e}\right)^{\frac{1}{2}} < \frac{B_e}{B_i}$$

Illustration by scatter plots Similar to Reeves 2011.

Balikhin et al., 2011

$cm^{-2}s^{-1}sr^{-1}KeV^{-1}$

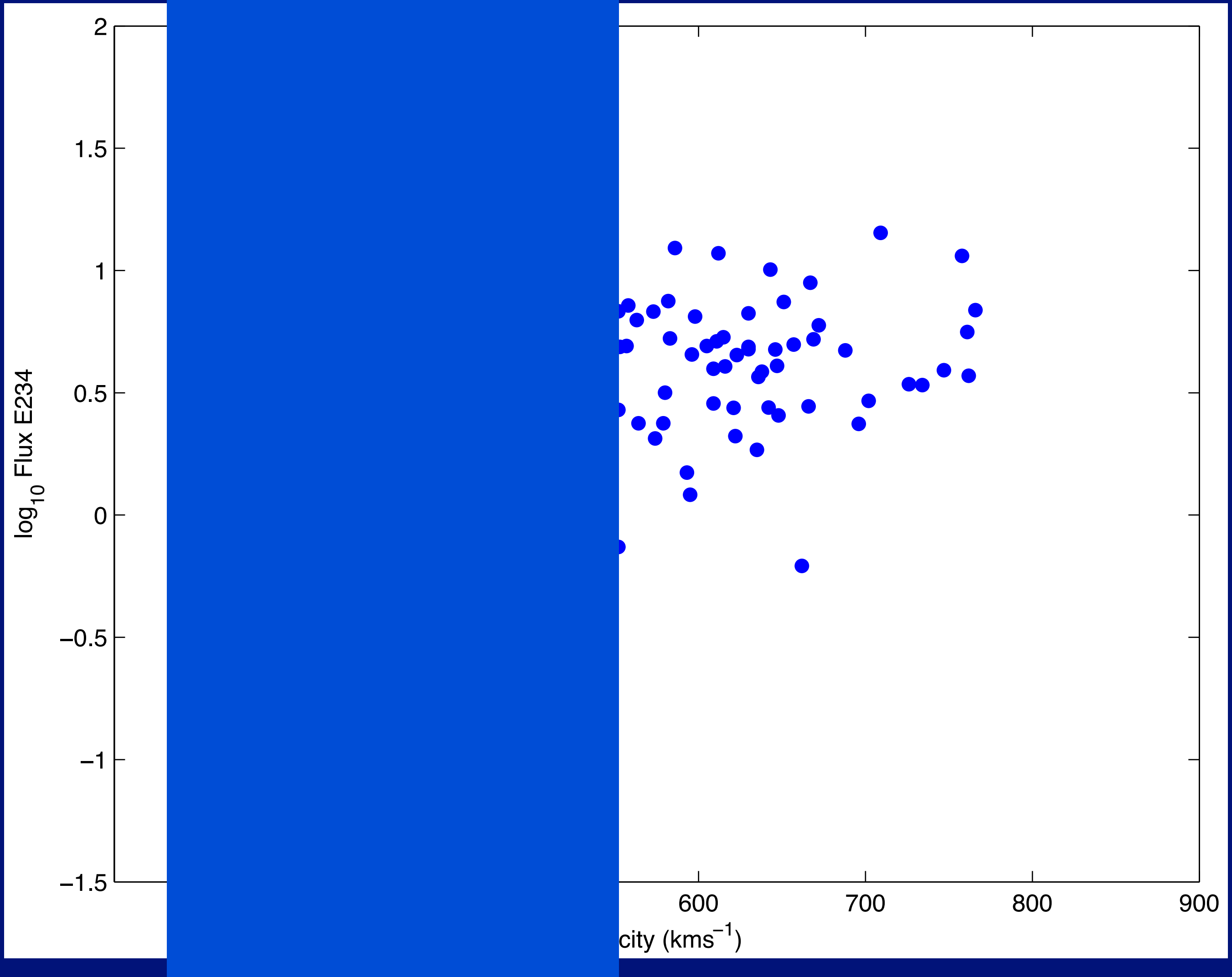

Illustration by scatter plots Similar to Reeves 2011.

Balikhin et al., 2011

$cm^{-2}s^{-1}sr^{-1}KeV^{-1}$

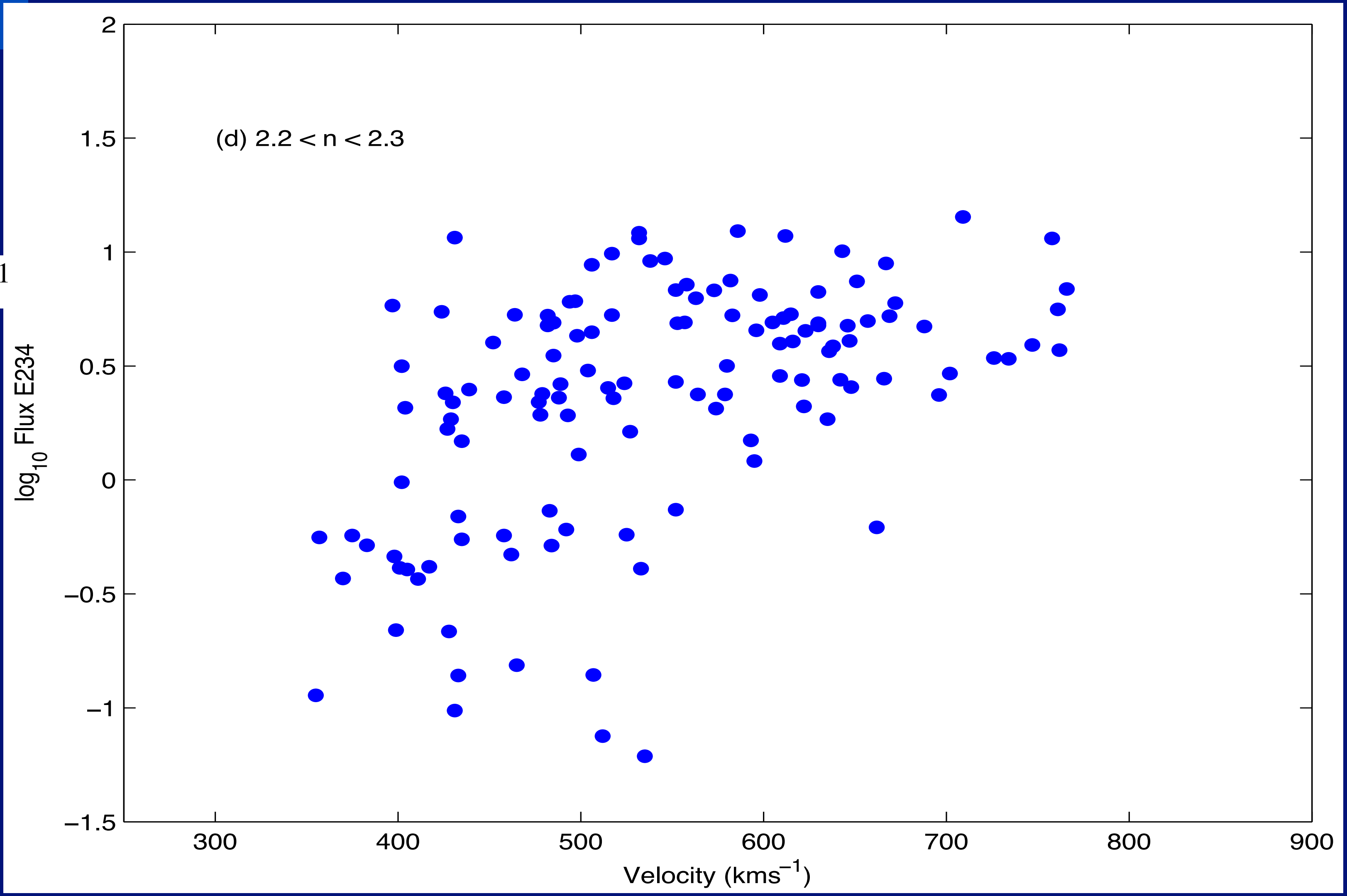

Illustration by scatter plots Similar to Reeves 2011.

Balikhin et al., 2011

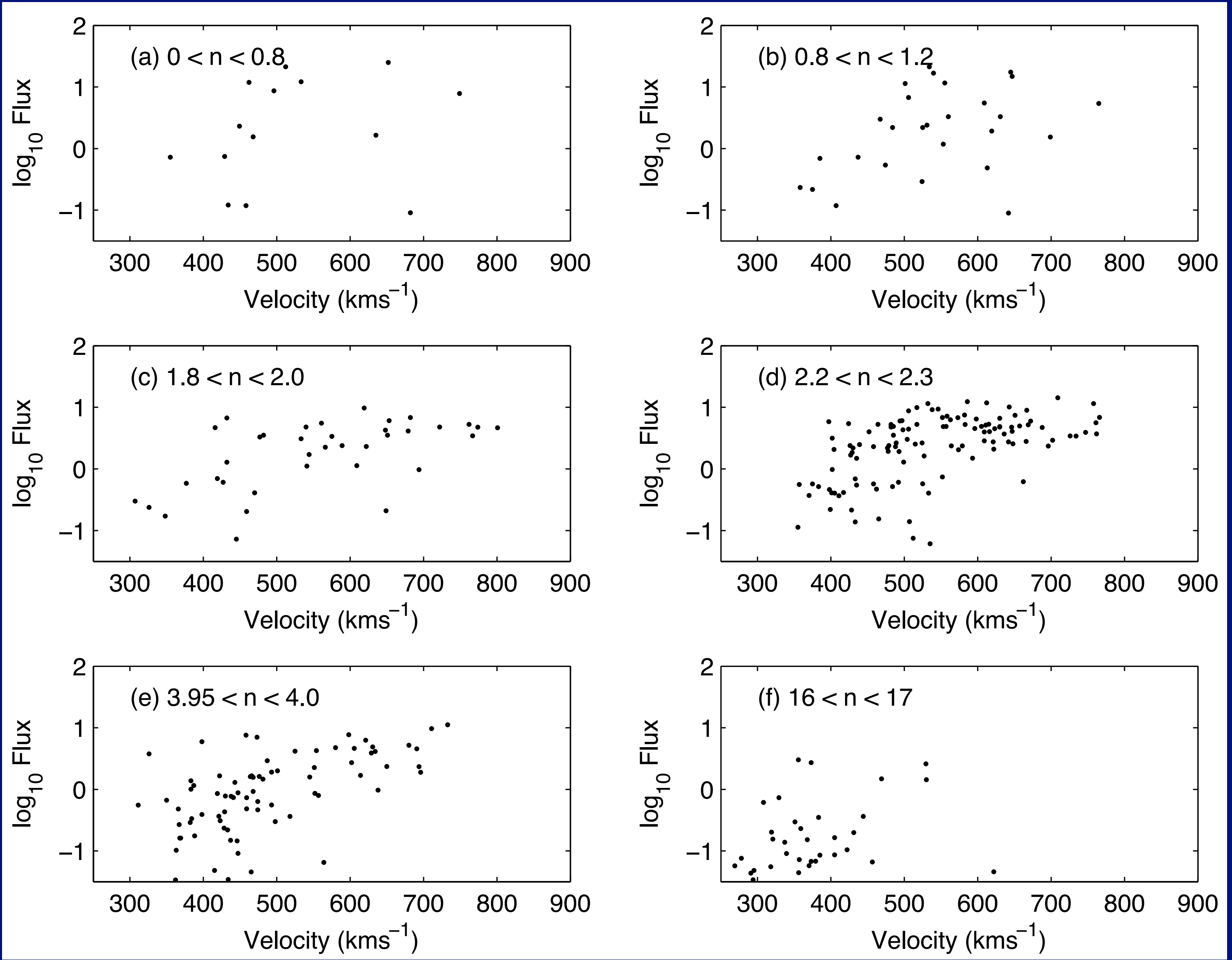

Earth's Radiation Belts

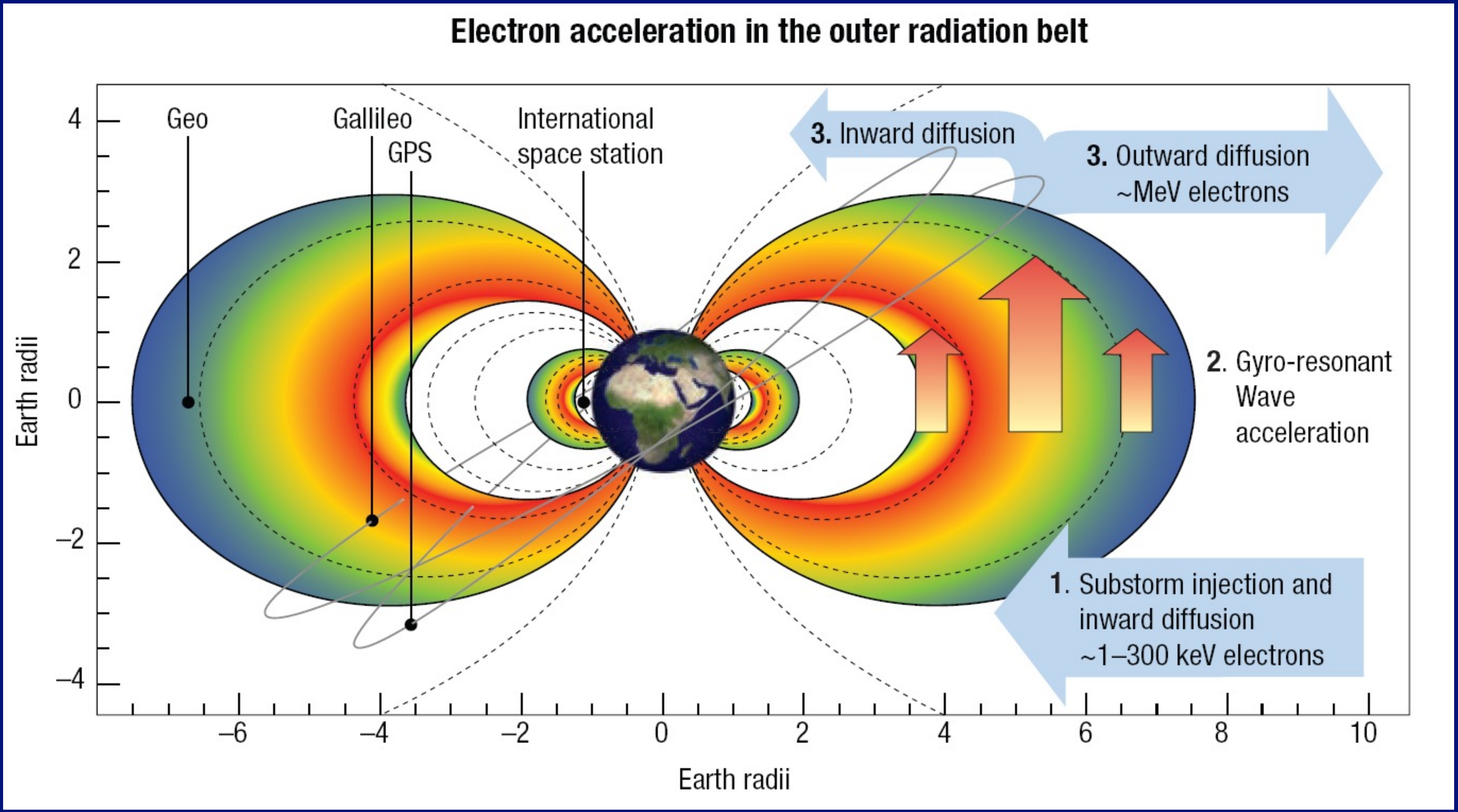

E_1, 24.1keV		
Term	**ERR (%)**	**Selected**
$V(t)$	96.928	8
$V^2(t)$	2.824	8
$n(t)$	0.082	8
$B_z(t)$	0.041	5
$VB_z(t)$	0.027	3

E_2, 31.7keV		
Term	**ERR (%)**	**Selected**
$V(t)$	96.944	8
$V^2(t)$	2.825	8
$n(t)$	0.071	8
$B_z(t)$	0.037	5
$VB_z(t)$	0.025	4

E_3, 41.6keV		
Term	**ERR (%)**	**Selected**
$V(t)$	96.968	8
$V^2(t)$	2.819	8
$n(t)$	0.057	8
$B_z(t)$	0.033	5
$VB_z(t)$	0.022	3

E_4, 62.5keV		
Term	**ERR (%)**	**Selected**
$V(t)$	97.014	8
$V^2(t)$	2.798	8
$n(t)$	0.035	8
$B_z(t)$	0.028	5
$nV(t)$	0.026	6

E_5, 90.0keV		
Term	**ERR (%)**	**Selected**
$V(t)$	97.062	8
$V^2(t)$	2.769	8
$nV(t)$	0.026	3
$VB_z(t)$	0.019	5
$B_z(t-1)$	0.019	7

E_6, 127.5keV		
Term	**ERR (%)**	**Selected**
$V(t)$	74.880	8
$V(t-1)$	22.252	7
$V^2(t)$	2.082	7
$V^2(t-1)$	0.646	7
$nV(t)$	0.020	5

E_7, 172.5keV		
Term	**ERR (%)**	**Selected**
$V(t-1)$	65.687	8
$V(t)$	31.563	7
$V^2(t-1)$	1.736	8
$V^2(t)$	0.876	6
$B_z(t-1)$	0.023	7

E_8, 270keV		
Term	**ERR (%)**	**Selected**
$V(t-1)$	97.476	8
$V^2(t-1)$	2.339	8
$B_z(t-1)$	0.022	7
$V(t)$	0.012	6
$pV(t)$	0.011	4

E_9, 407.5keV		
Term	**ERR (%)**	**Selected**
$V(t-1)$	84.116	8
$V(t-2)$	13.726	4
$V^2(t-1)$	1.626	8
$V^2(t-2)$	0.247	4
$nV(t)$	0.031	4

E_{10}, 625keV		
Term	**ERR (%)**	**Selected**
$V(t-1)$	75.876	8
$V(t-2)$	22.275	3
$V^2(t-1)$	0.610	4
$V(t-4)$	0.243	6
$V^2(t-2)$	0.215	3

E_{11}, 925keV		
Term	**ERR (%)**	**Selected**
$V(t-2)$	96.162	8
$n(t)$	0.279	2
$V(t-4)$	0.238	7
$n(t-4)$	0.197	2
$p(t)$	0.195	4

E_{12}, 1.3MeV		
Term	**ERR (%)**	**Selected**
$V^2(t-2)$	76.508	7
$nV(t-1)$	2.211	3
$nV(t)$	1.900	2
$V^2(t-3)$	1.692	2
$V^2(t-4)$	1.384	7

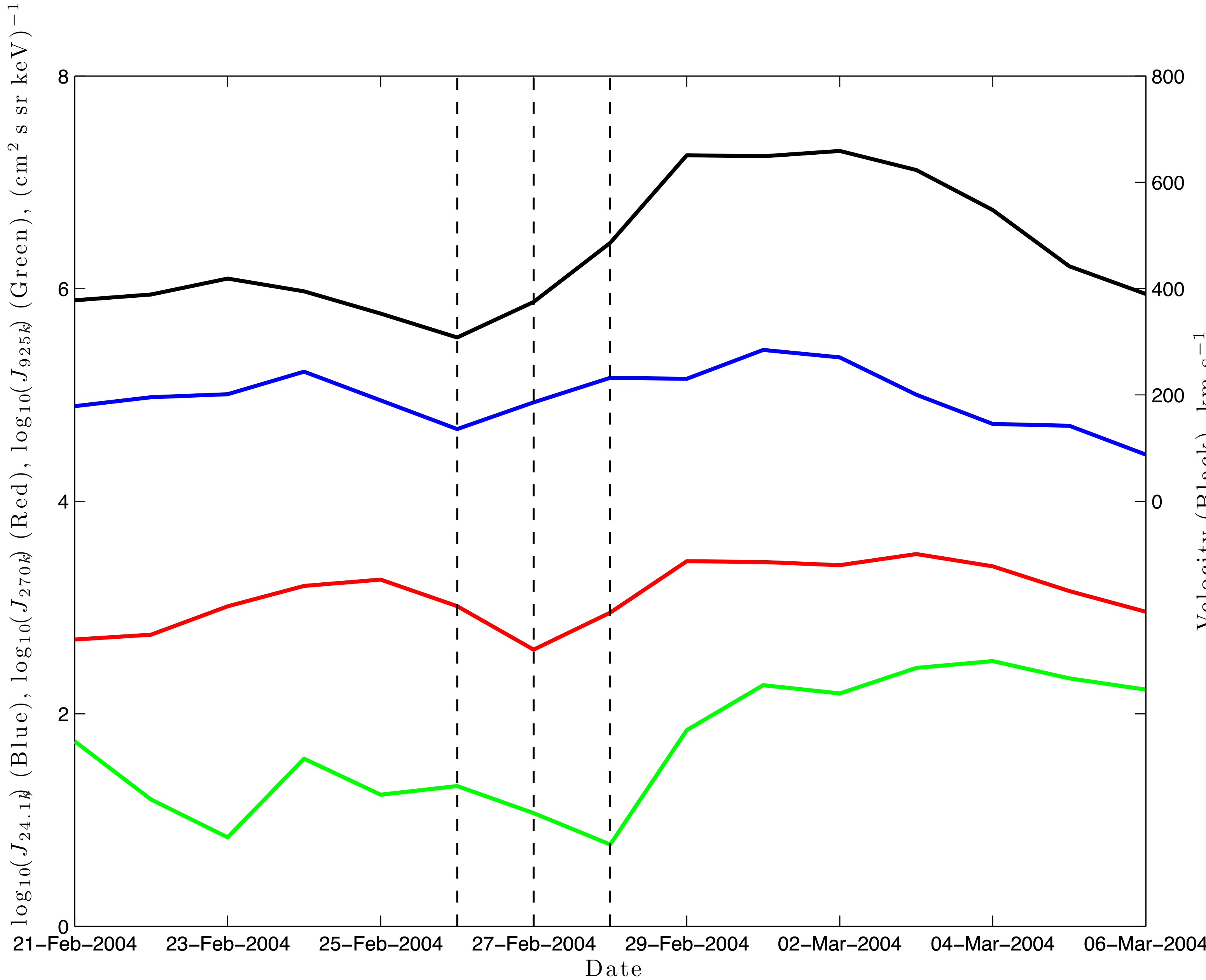

$\log_{10}(J_{24.1k})$ (Blue), $\log_{10}(J_{270k})$ (Red), $\log_{10}(J_{925k})$ (Green), $(\mathrm{cm}^2\ \mathrm{s\ sr\ keV})^{-1}$
Velocity (Black), km s^{-1}
Date
0
2
4
6
8
0
200
400
600
800
21–Feb–2004
23–Feb–2004
25–Feb–2004
27–Feb–2004
29–Feb–2004
02–Mar–2004
04–Mar–2004
06–Mar–2004

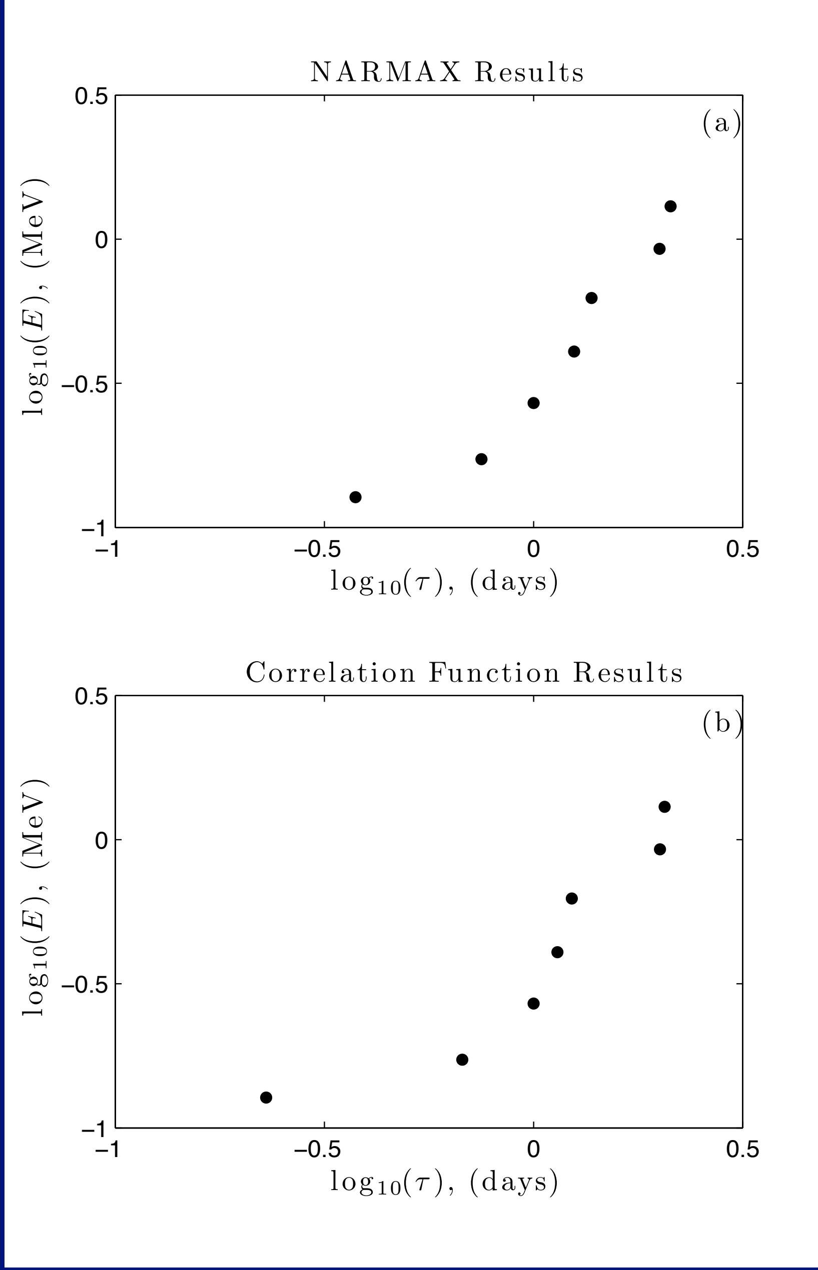

Energy diffusion equation Horne et al., 2005:

$$\left\langle \frac{\partial F}{\partial t} \right\rangle = \frac{\partial}{\partial E}\left[A(E)\langle D_{EE}\rangle \frac{\partial}{\partial E}\left(\frac{F}{A(E)}\right)\right] - \frac{F}{\tau_L},$$

$$A = (E + E_0)(E + 2E_0)^{\frac{1}{2}} E^{\frac{1}{2}},$$

$$F(E, \alpha_{eq}) = \frac{A(E)}{c^3} f(\mathbf{p}, \alpha_{eq}) = \frac{(E + E_0)}{cE^{\frac{1}{2}}(E + 2E_0)^{\frac{1}{2}}} J(E, \alpha_{eq}), \quad (11)$$

$$\frac{\partial F}{\partial t} = D\frac{\partial}{\partial E}\left[E^\beta \frac{\partial}{\partial E}\left[\frac{F}{E^\beta}\right]\right],$$

$$F = fE^{\frac{\beta+1}{2}}$$

$$\frac{\partial f}{\partial t} = \frac{\partial^2}{\partial E^2}f + \frac{1}{E}\frac{\partial f}{\partial E} - \frac{b^2}{E^2}f,$$

$$f = T(t)Y(E)$$

$$\frac{1}{T}\frac{dT}{dt} = -k^2.$$

$$\frac{d^2Y}{dE^2} + \frac{1}{E}\frac{dY}{dE} + (k^2 - \frac{b^2}{E^2})Y = 0$$

$$Y(E) = c_1(k)J_b(kE) + c_2(k)N_b(kE)$$

$$F = \int_0^\infty dk \exp\left(-k^2Dt\right)C(k)J_b(kE)E^{\frac{\beta+1}{2}}$$

$$F_0(E)E^{-\frac{\beta}{2}} = \int_0^\infty dk\sqrt{kE}C(k)J_b(kE)$$

$$C(k) = \int_0^\infty dE\sqrt{kE}F_0(E)E^{-\frac{\beta}{2}}J_b(kE)$$

E << mc^2

$$F = CEt^{-5/4}\exp\left(-\frac{E^2}{4DE_0^2t)}\right)$$

E >> mc^2

$$F = CE^2t^{-3/2}\exp\left(-\frac{E^2}{4DE_0^2t}\right)$$

$E \ll mc^2$

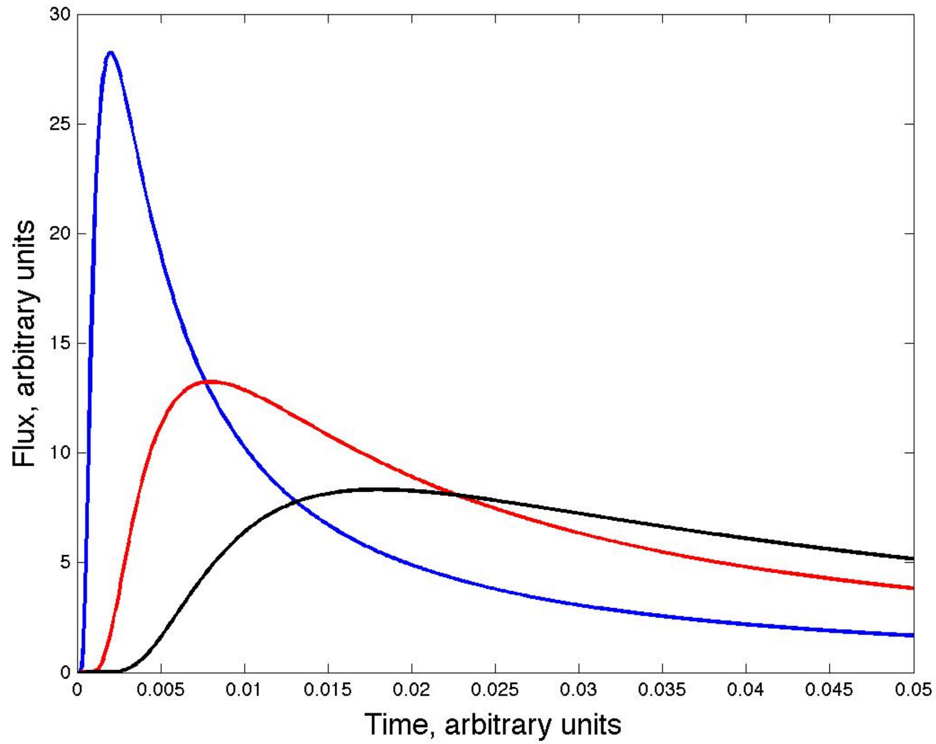

$E \gg mc^2$

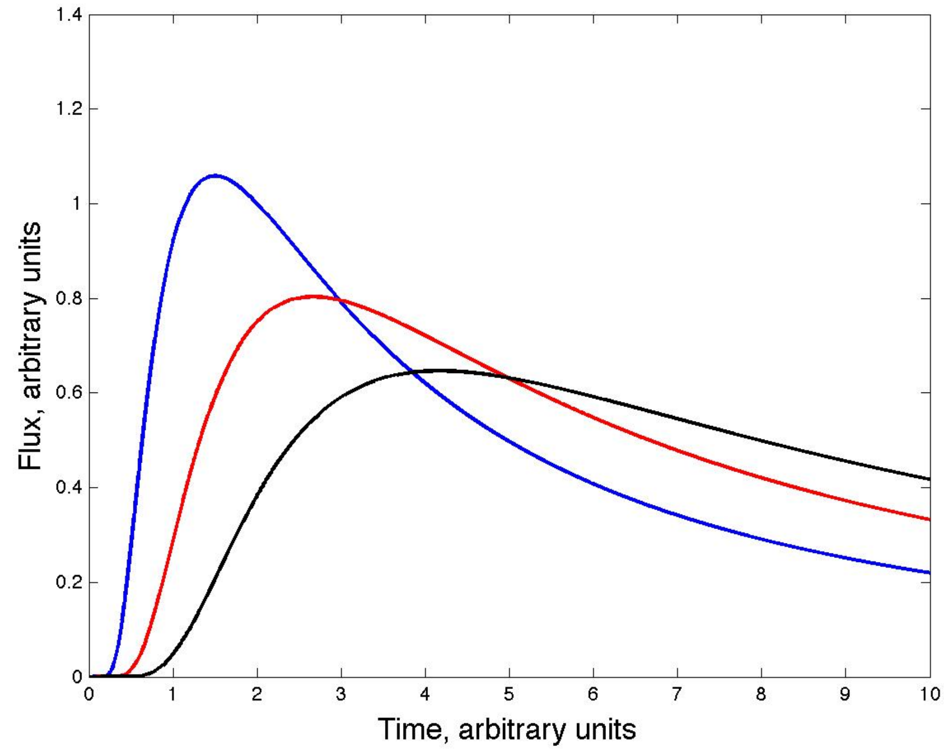

$$t_{E=0.1} : t_{E=0.2} : t_{E=0.3} = 1 : 4.10 : 9.10$$

$$t_{E=3} : t_{E=4} : t_{E=5} = 1 : 1.78 : 2.77$$

$$F(E, \alpha_{eq}) = \frac{A(E)}{c^3} f(\mathbf{p}, \alpha_{eq}) = \frac{(E + E_0)}{cE^{\frac{1}{2}}(E + 2E_0)^{\frac{1}{2}}} J(E, \alpha_{eq}), \quad (11)$$

Horne et el., 2005

The one day ahead forecasts of the relativistic electron fluxes with energies greater than 2 MeV at GEO has been developed in Sheffield and is available in real time:

http://ssg.group.shef.ac.uk/ssg2013/UOSSW/2MeV_EF.html

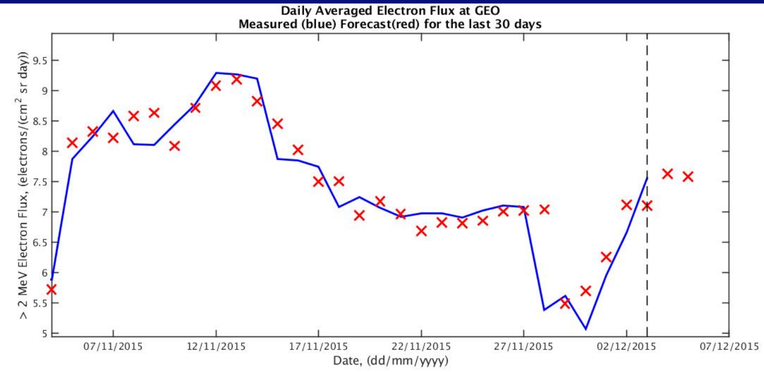

Past 90 days

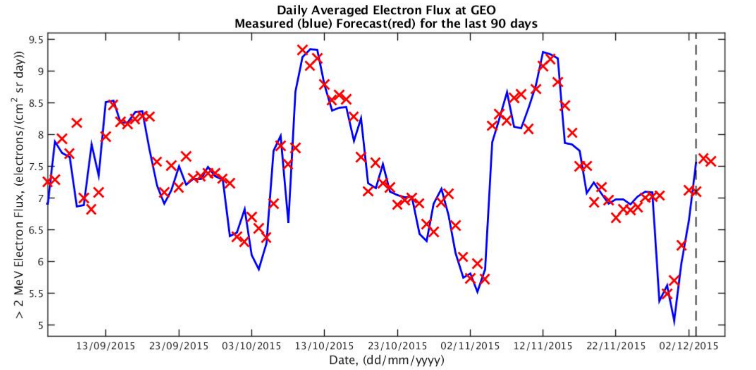

Past 200 days

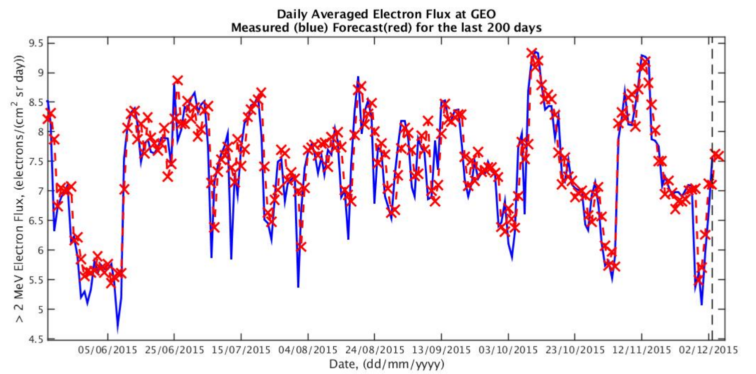

NOAA REFM Forecast

SPACE WEATHER PREDICTION CENTER
NATIONAL OCEANIC AND ATMOSPHERIC ADMINISTRATION

Thursday, December 03, 2015 09:34:58 UTC

HOME   ABOUT SPACE WEATHER   PRODUCTS AND DATA   DASHBOARDS   MEDIA AND RESOURCES

SUBSCRIBE   ANNUAL MEETING   FEEDBACK

Home > Products and Data > Models > Relativistic Electron Forecast Model

Search

CURRENT SPACE WEATHER CONDITIONS on NOAA Scales

R	S	G
none	none	none

RELATIVISTIC ELECTRON FORECAST MODEL

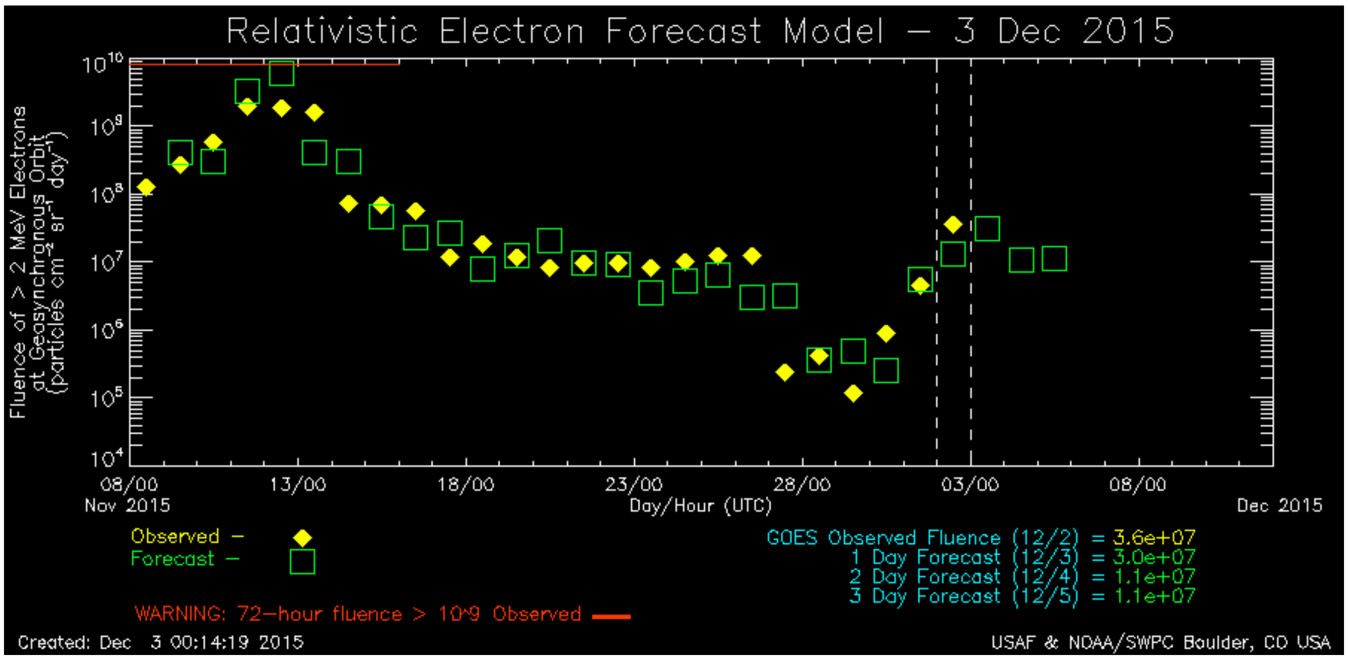

Comparison of REFM and SNB^{3}GEO Forecasts (01.03.2012-03.07.2014)

Balikhin, Rodriguez,Boynton, Walker,Aryan, Sibeck, Billings (submitted to SW 2015)

$$PE = 1 - \frac{1}{N}\sum \frac{(Y(t) - Ym(t))^2}{\mathrm{var}(Y)}$$

$$C_{cor} = \frac{1}{N}\sum \frac{(Y(t) - \langle Y(t)\rangle)(Ym(t) - \langle Ym(t)\rangle)}{\sqrt{\mathrm{var}(Ym)\mathrm{var}(Y)}}$$

Comparison of REFM and SNB^{3}GEO Forecasts

Balikhin, Rodriguez, Boynton, Walker, Aryan, Sibeck Billings, submitted to SW 2015

Model	Prediction Efficiency Flux	Correlation Flux	Prediction Efficiency Log Flux	Correlation Log Flux
REFM	-1.31	0.73	0.70	0.85
SNB^{3}GEO	0.63	0.82	0.77	0.89

Comparison of REFM and SNB^{3}GEO Forecasts

Balikhin, Rodriguez, Boynton, Walker, Aryan, Sibeck Billings, submitted to SW 2015

Table 2. Contingency tables and Heidke skill scores for the REFM predictions.

Fluence ($\mathrm{cm^{-2}sr^{-1}day^{-1}}$)	$> 10^8$		$> 10^{8.5}$		$> 10^9$	
REFM HSS	0.666		0.482		0.437	
Observation:	Yes	No	Yes	No	Yes	No
Forecast						
Yes	86	22	23	22	4	7
No	43	510	21	595	3	647

Table 3. Contingency tables and Heidke skill scores for the SNB^{3}GEO predictions.

Fluence ($\mathrm{cm^{-2}sr^{-1}day^{-1}}$)	$> 10^8$		$> 10^{8.5}$		$> 10^9$	
SNB^{3}GEO HSS	0.738		0.634		0.612	
Observation:	Yes	No	Yes	No	Yes	No
Forecast						
Yes	106	33	31	19	4	2
No	23	499	13	598	3	652

$$S = \frac{2(xw - yz)}{y^2 + z^2 + 2xw + (y+z)(x+w)}$$

The one day ahead forecasts of the relativistic electron fluxes with energies greater than 2 MeV at GEO has been developed in

Real time forecast of the >2 MeV electron flux at geosynchronous orbit

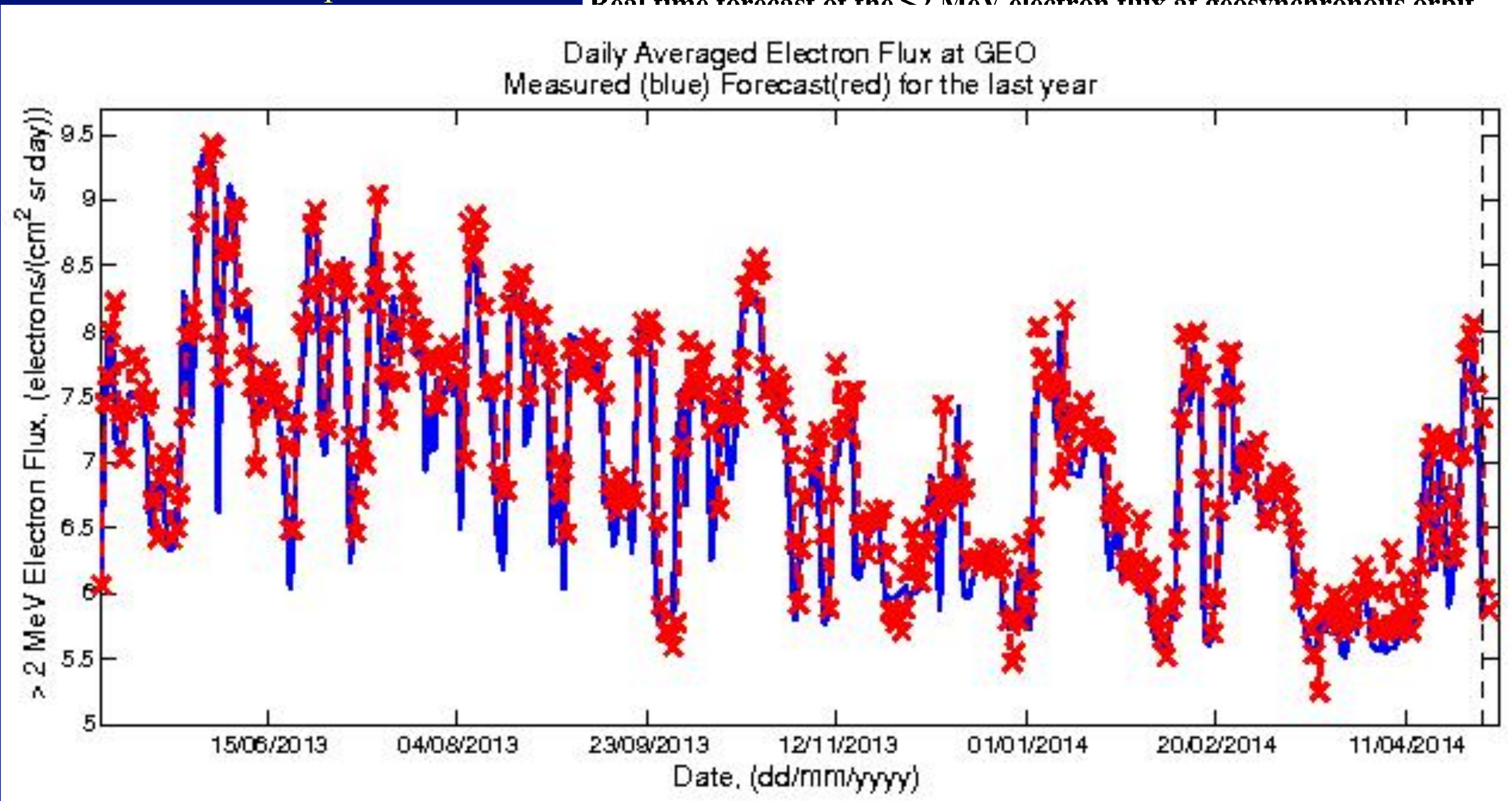

Extending SNB^{3}GEO to lower energies

Model	Forecast Time (hours)	PE (%)	CC (%)	Period
40-50 keV	10	66.9	82.0	01.03.2013-28.02.2015
50-100 keV	12	69.2	83.5	01.03.2013-28.02.2015
100-200 keV	16	73.2	85.6	01.03.2013-28.02.2015
200-350 keV	24	71.6	84.9	01.03.2013-28.02.2015
350-300 keV	24	73.6	85.9	01.03.2013-28.02.2015
> 800 keV	24	72.1	85.1	01.01.2011-28.02.2015
> 2MeV	24	82.3	90.9	01.0.12011-28.02.2015

Extending SNB^{3}GEO to lower energies

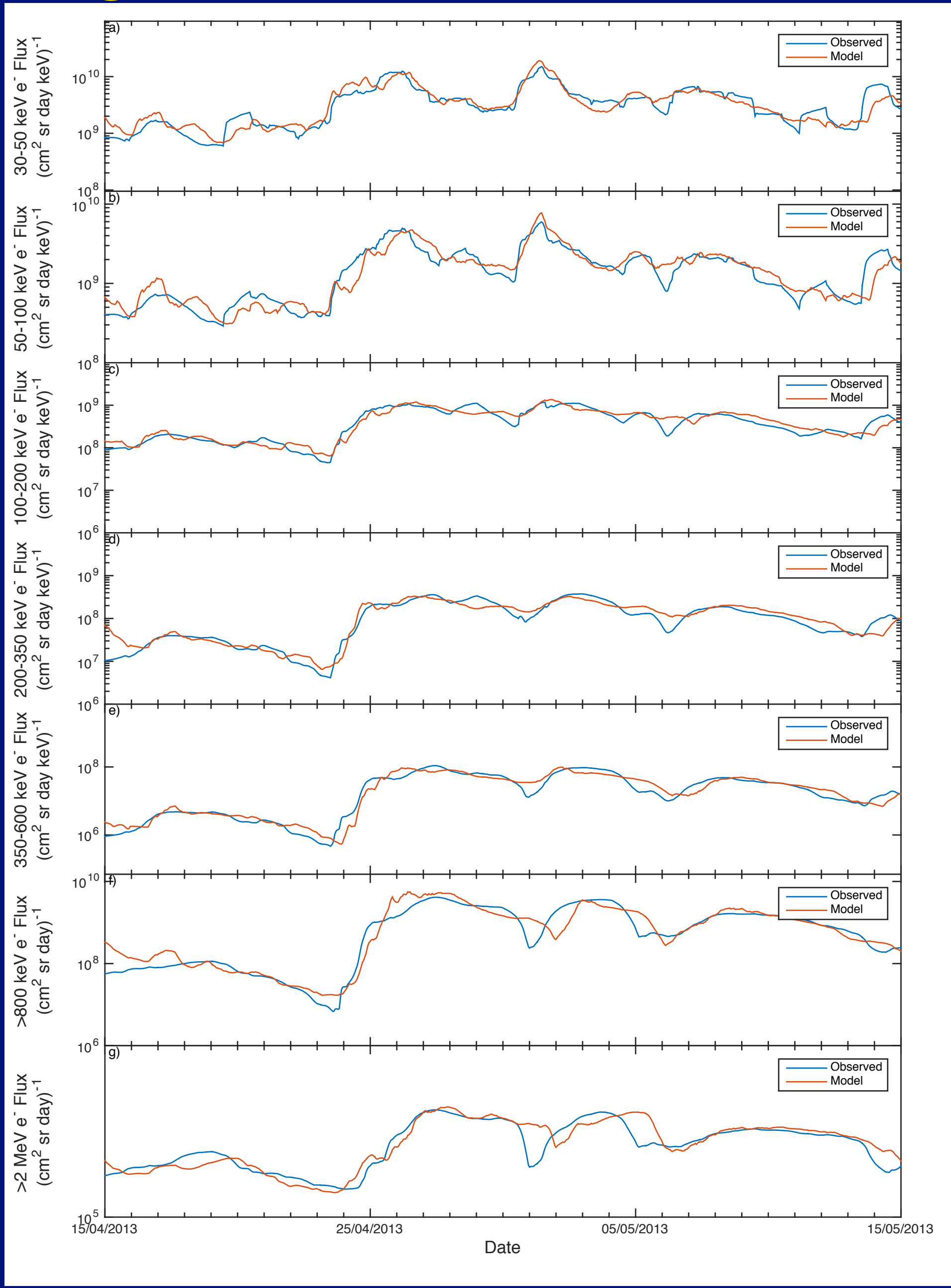

PROGRESS: wave models

- Statistical Wave models and physics of wave particle interaction

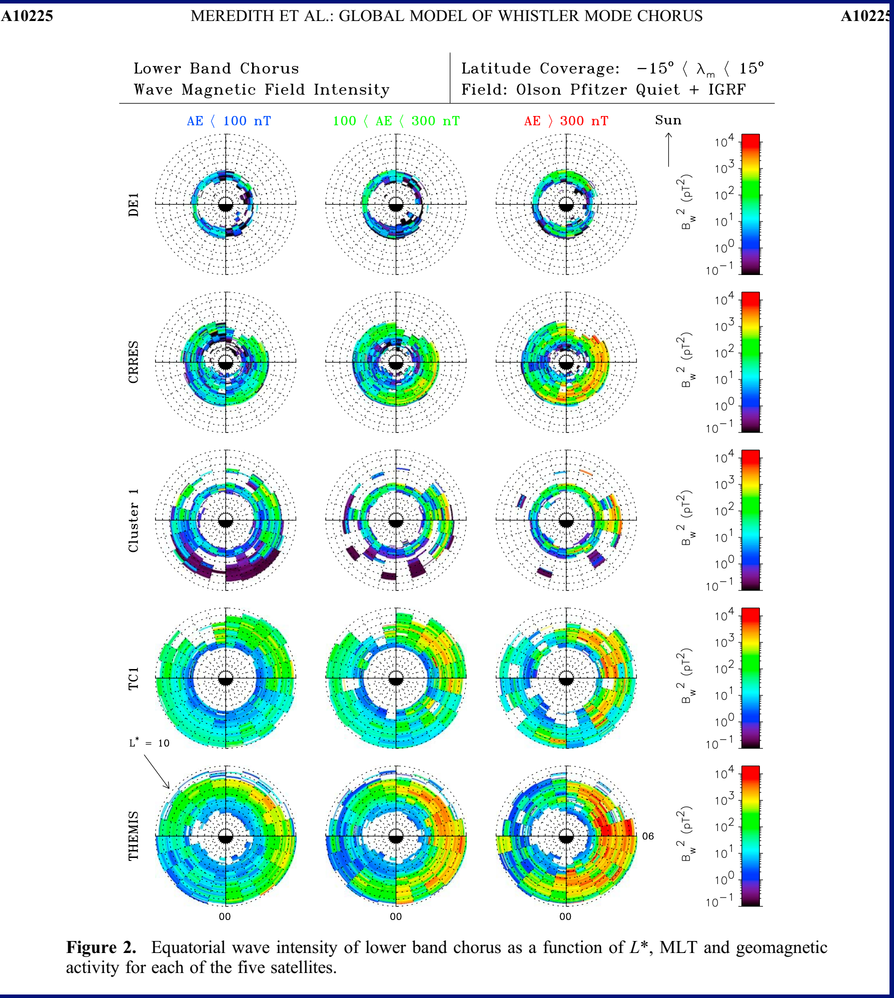

Figure 2. Equatorial wave intensity of lower band chorus as a function of L^*, MLT and geomagnetic activity for each of the five satellites.

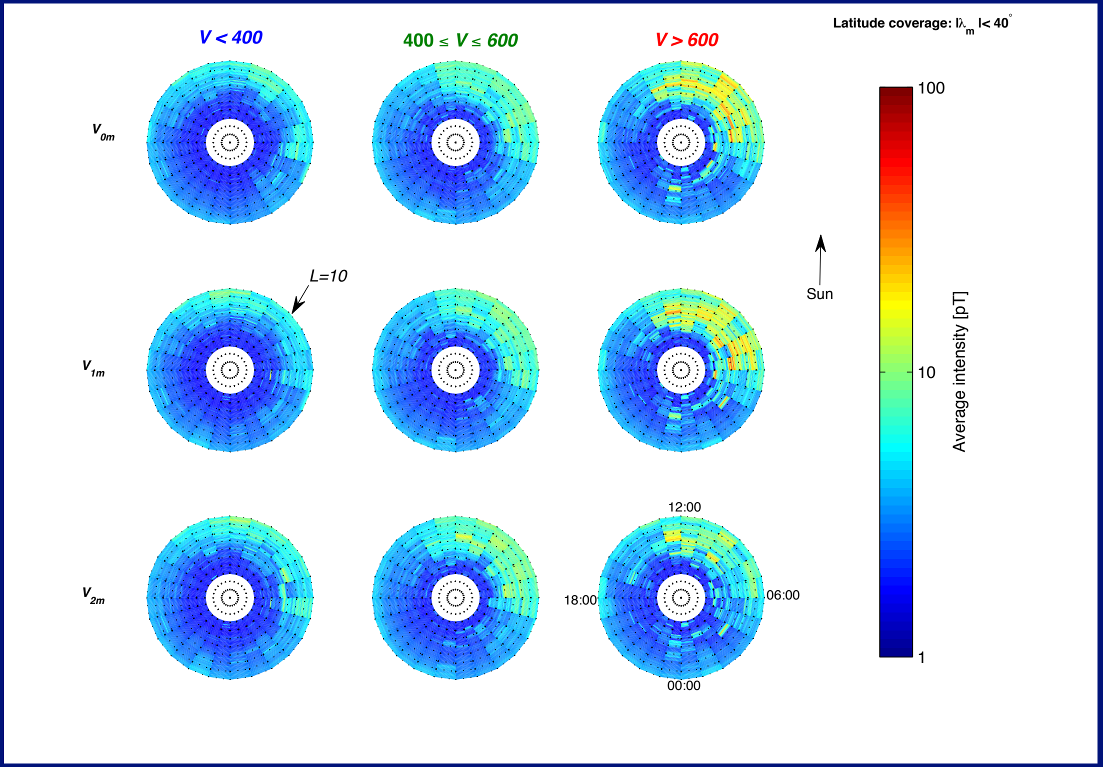

PROGRESS: wave models LB Chorus

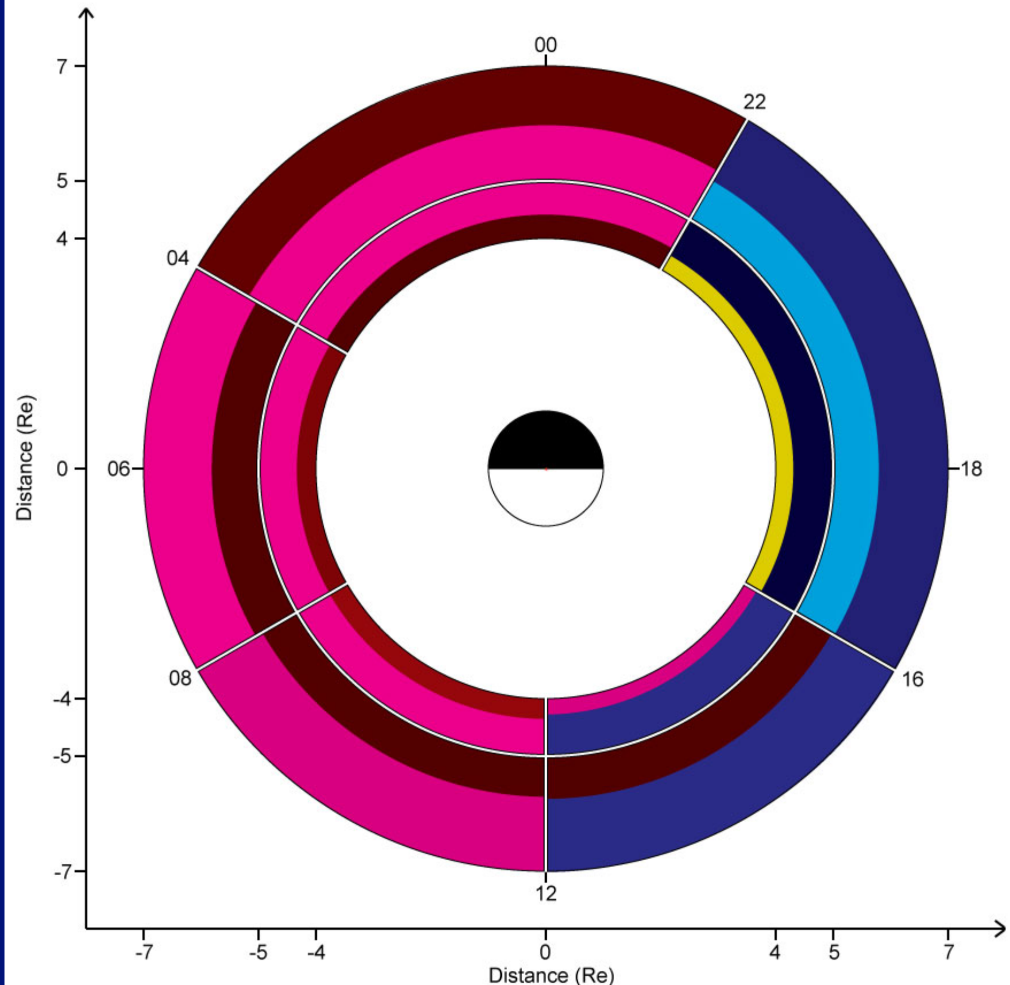

Time lag (hours) / Input	1	2	3	4	5	6	7	8	9	10
Velocity										
Density										
Pressure										
IMF Factor										
Dst Index										
AE Index										

PROGRESS: wave models Hiss

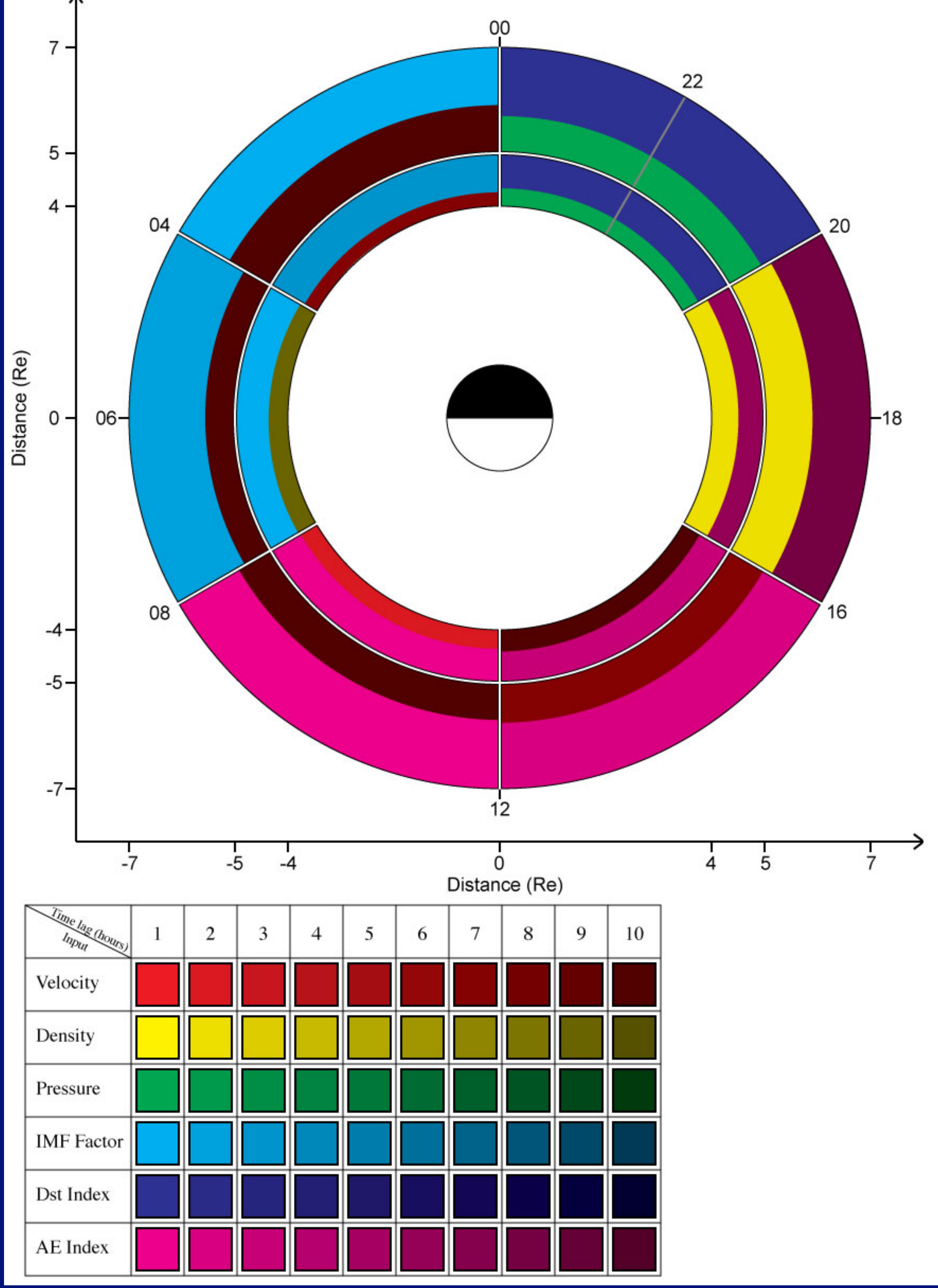

PROGRESS: wave models EMW

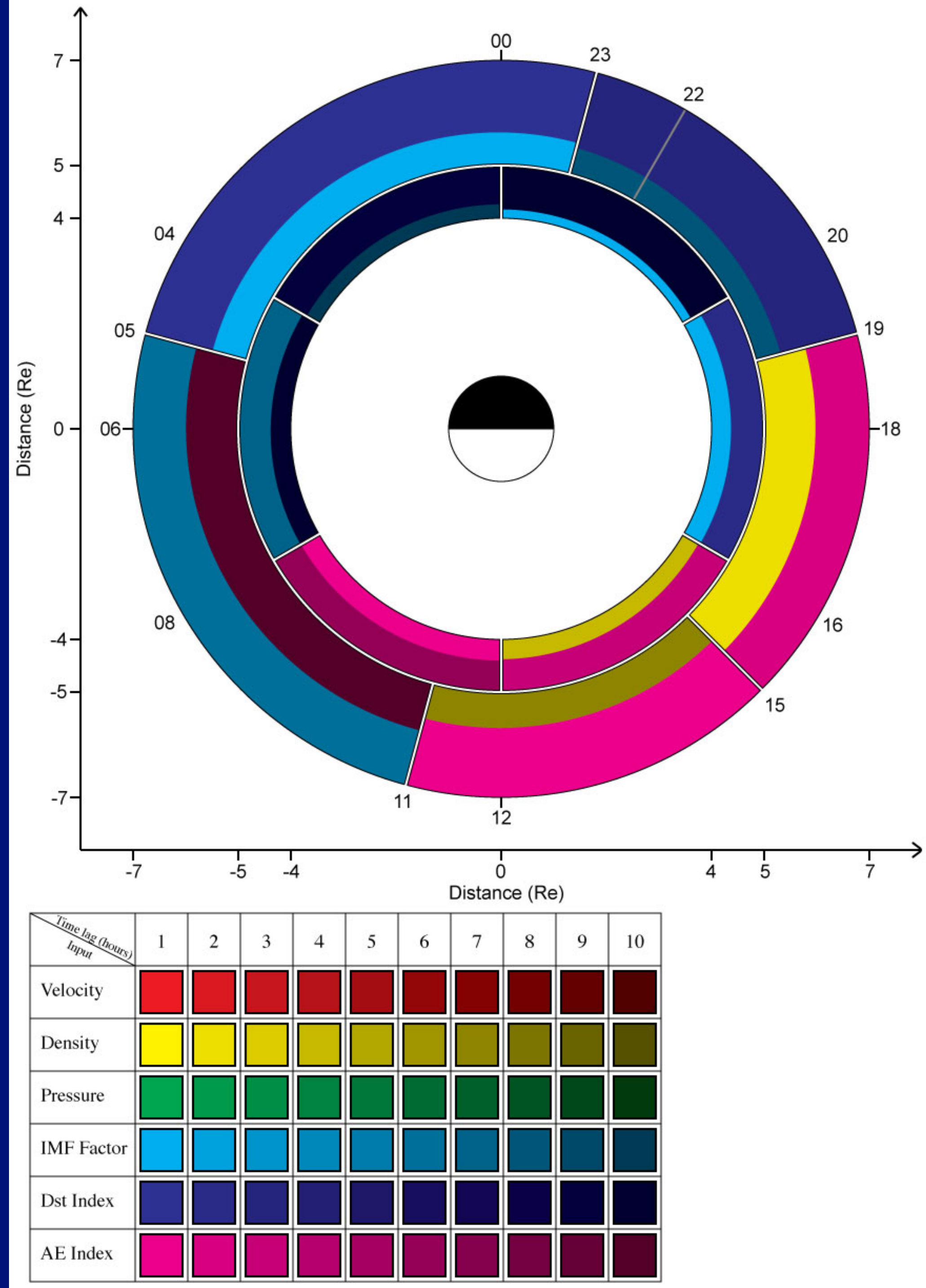

EMW Spectral Observations

Most studies of the amplitudes of magnetosonic waves assume a continuous spectrum and hence the validity of the quasi-linear theory

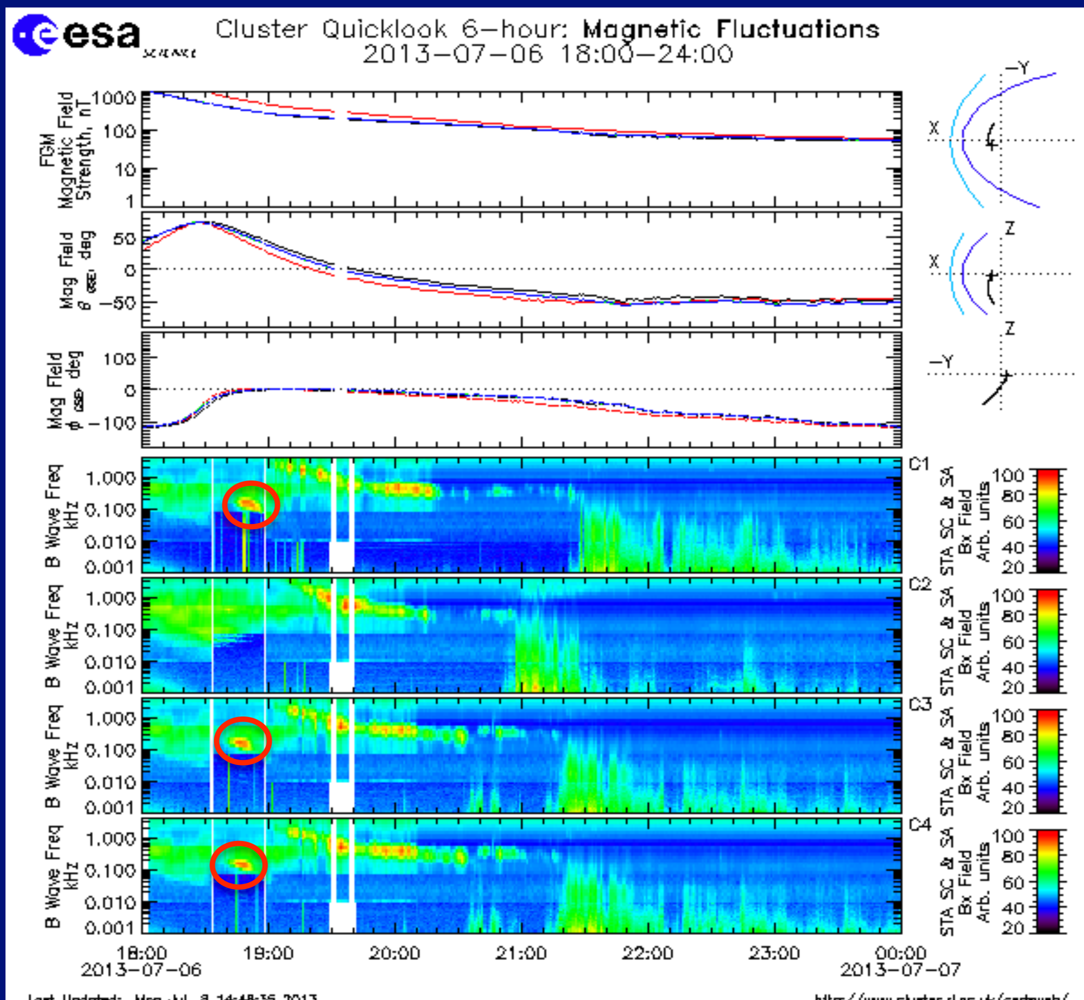

The figure shows an overview of the STAFF spectrum analyser observations on July 6th, 2013. Occurrences o Equatorial magnetosonic waves are indicated by the red circles.

The waves appear continuous in frequency space. Thus, quasi-linear theory is used to estimate their effects on electron acceleration and loss processes.

Balikhin, Shprits, Walker et al., Nature Comm, 2015

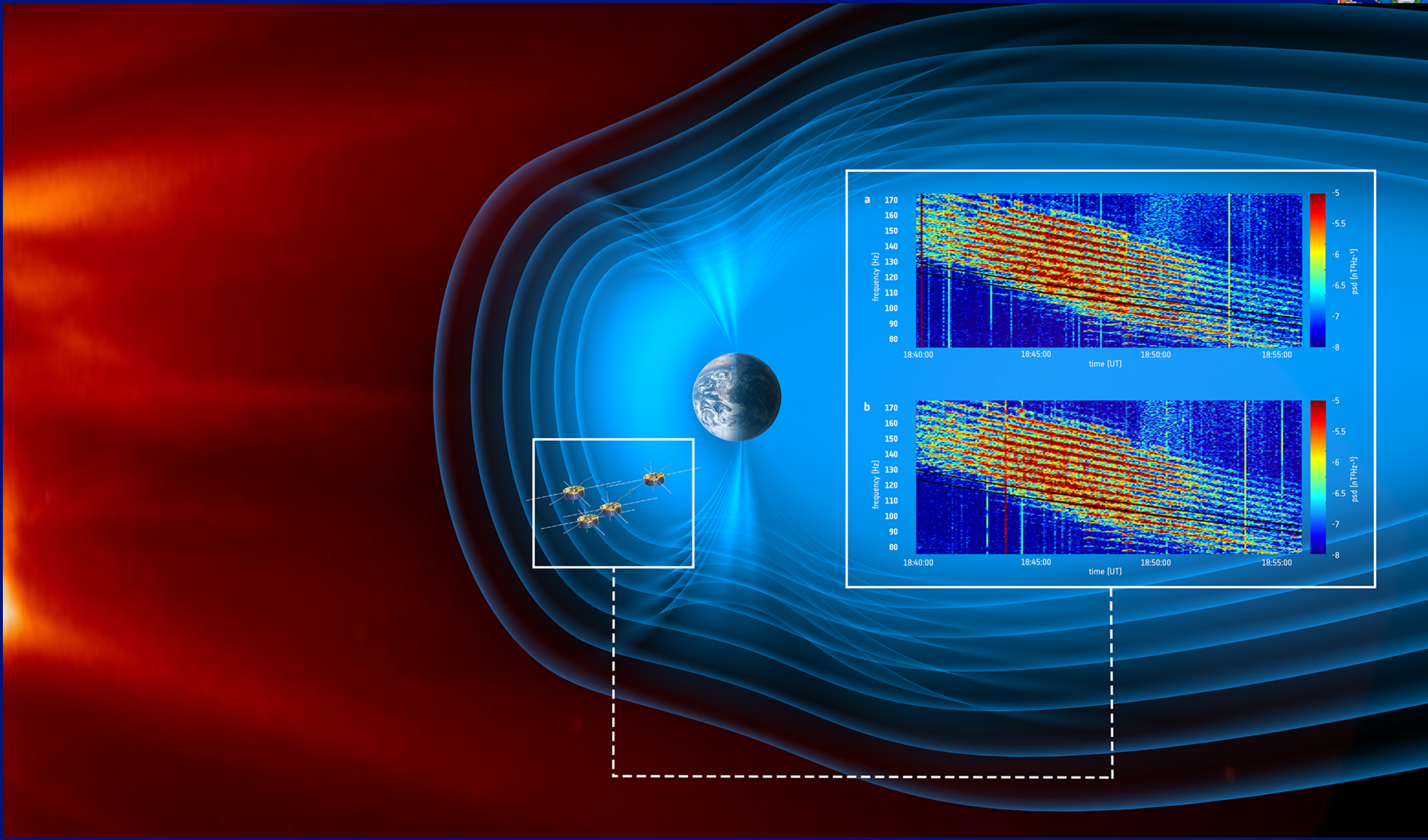

Balikhin, Shprits, Walker et al., Nature Comm, 2015

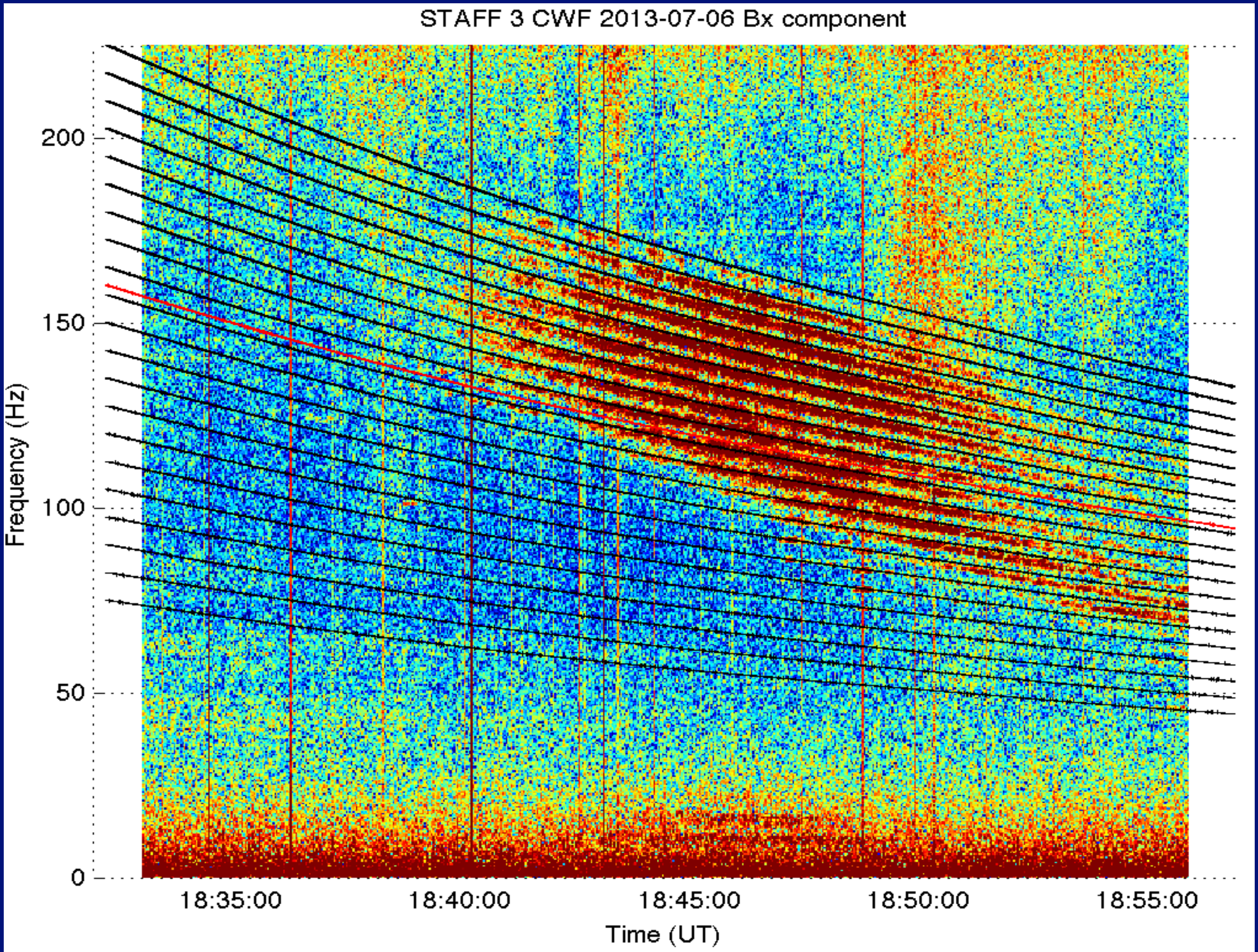

Conclusion:

1)According to our knowledge SNB^{3}GEO model provides the most accurate forecast of daily averaged fluxes of energetic electrons (>2MeV)

2) The model that extends the forecast from 1 per day to 1 per hour is developed and undergoing assessment now.

Table 2. Various Possible Viscous Solar Wind Coupling Functions, Ranked According to Their Ability to Predict Variance in 10 Magnetospheric State Variables

Rank, f	Λ_c	Dst	AE	AU	Goes	Kp	Auro	b2i	Φ_{PC}	AL	$\Sigma r^2/n$
1. $n^{1/2}v^2$	−0.364	−0.500	0.469	0.430	−0.325	0.670	0.510	−0.520	0.319	−0.225	22.3%
2. $n^{1/3}v^2$	−0.371	−0.497	0.458	0.389	−0.353	0.678	0.512	−0.460	0.324	−0.250	21.8%
3. $n^{1/2}v^3$	−0.363	−0.517	0.452	0.383	−0.340	0.653	0.515	−0.449	0.317	−0.236	21.1%
4. $n^{1/6}v^2$	−0.353	−0.460	0.416	0.330	−0.347	0.628	0.471	−0.382	0.294	−0.254	18.5%
5. nv^3	−0.331	−0.507	0.425	0.421	−0.260	0.549	0.488	−0.516	0.272	−0.153	18.5%
6. $nv^{5/2}$	−0.312	−0.457	0.383	0.401	−0.239	0.525	0.448	−0.511	0.249	−0.124	16.3%
7. $v^{4/3}$	−0.374	−0.408	0.372	0.277	−0.321	0.547	0.402	−0.314	0.252	−0.250	14.7%
8. v	−0.324	−0.406	0.374	0.279	−0.321	0.537	0.399	−0.315	0.254	−0.251	14.7%
9. $v^{3/2}$	−0.321	−0.408	0.372	0.276	−0.319	0.549	0.404	−0.312	0.251	−0.249	14.7%
10. v^2	−0.317	−0.409	0.369	0.272	−0.311	0.547	0.407	−0.310	0.247	−0.246	14.4%
11. $v^{2/3}$	−0.325	−0.405	0.374	0.281	−0.311	0.503	0.396	−0.316	0.255	−0.252	14.4%
12. $v^{1/2}$	−0.325	−0.403	0.374	0.282	−0.294	0.465	0.395	−0.316	0.255	−0.252	14.0%
13. p	−0.277	−0.373	0.316	0.357	−0.202	0.469	0.391	−0.474	0.217	−0.085	12.5%
14. $p^{2/3}$	−0.272	−0.321	0.326	0.365	−0.199	0.486	0.377	−0.485	0.228	−0.101	12.4%
15. $p^{1/2}$	−0.267	−0.295	0.329	0.367	−0.194	0.482	0.366	−0.486	0.231	−0.108	12.2%
16. $p^{1/3}$	−0.193	−0.269	0.331	0.366	−0.186	0.463	0.353	−0.485	0.231	−0.115	11.7%
17. $p^{3/2}$	−0.274	−0.427	0.288	0.331	−0.183	0.394	0.397	−0.431	0.190	−0.057	11.1%
18. p^2	−0.257	−0.420	0.250	0.292	−0.150	0.288	0.387	−0.351	0.159	−0.031	8.5%
19. nv	−0.163	−0.149	0.143	0.221	−0.089	0.287	0.253	−0.325	0.136	0.004	4.0%
20. n	−0.041	0.030	0.001	0.093	0.033	0.103	0.122	−0.172	0.058	0.070	0.6%

Solar Wind Magnetosphere“Coupling Functions”

X(t) ⇒ x^2 ⇒ Y(t)

5% Noise

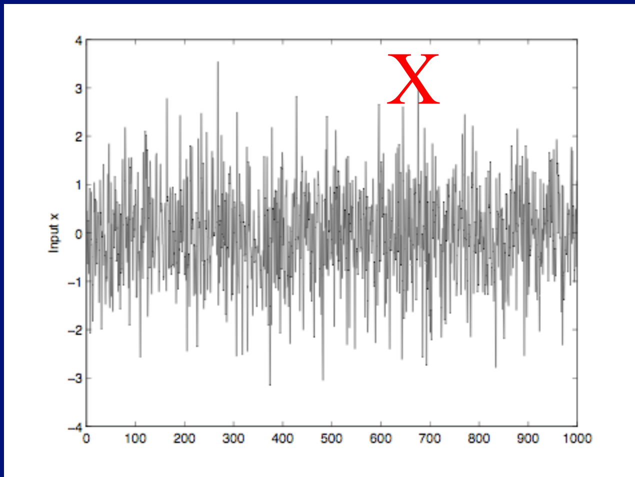

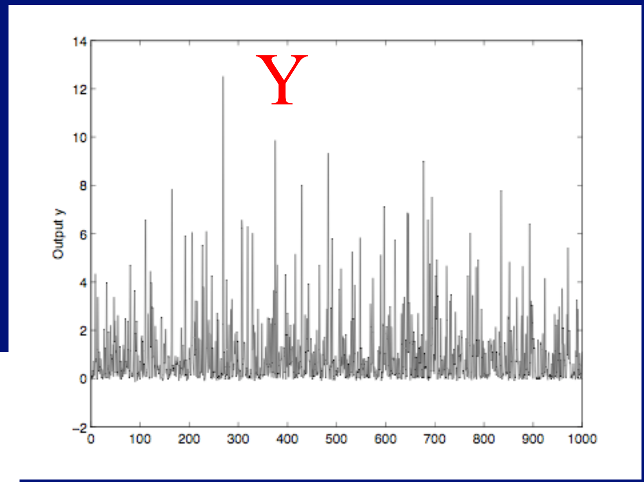

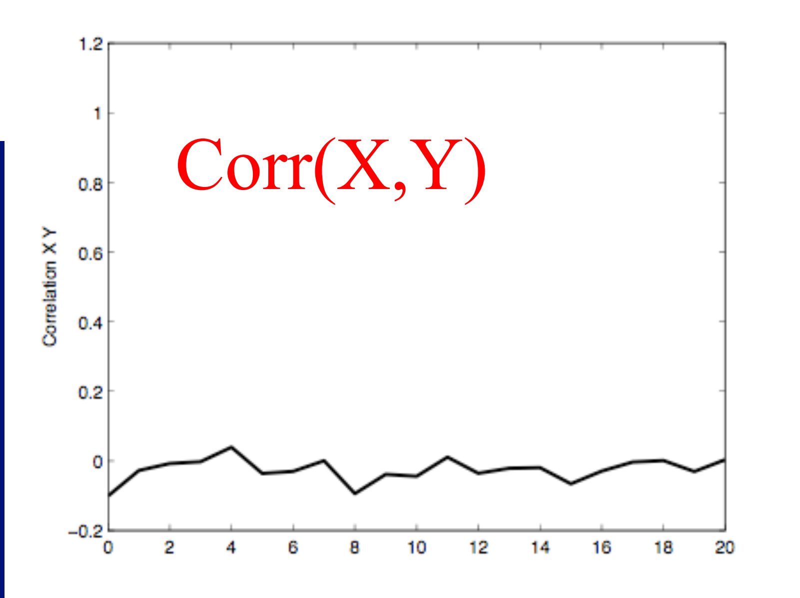

(X, Y)

(X^2, Y)

....

(X^k, Y)

(X^{k+1}, Y)

....

$$y(t)=x(t)^2+0.5x(t-1)^4+y(t-1)\,x(t-1)$$

Previously proposed coupling functions

1. $I_B = VB_s$ by *Burton et al.* [1975]
2. $\varepsilon = VB^2\sin^4(\theta/2)$, by *Perreault and Akasofu* [1978]
3. $I_W = VB_T\sin^4(\theta/2)$ by *Wygant et al.* [1983]
4. $I_{SR} = p^{1/2}VB_T\sin^4(\theta/2)$ by *Scurry and Russell* [1991]
5. $I_{TL} = p^{1/2}VB_T\sin^6(\theta/2)$ by *Temerin and Li* [2006]
6. $I_N = V^{4/3}B_T^{2/3}\sin^{8/3}(\theta/2)$ by *Newell et al.* [2007]
7. $I_V = n^{1/6}V^{4/3}B_T\sin^4(\theta/2)$ by *Vasyliunas et al.* [1982]

Coupling Function	NERR
$p^{1/2}VB_T\sin^6(\theta/2)(t\text{-}1)$	31.32
$VB_s(t\text{-}1)$	12.76
$n^{1/6}V^{4/3}B_T\sin^4(\theta/2)(t\text{-}1)$	10.30
$p^{1/2}VB_T\sin^4(\theta/2)(t\text{-}1)$	8.37
$D_{st}(t\text{-}2)$	7.23

$p^{1/2}V^2B_T\sin^6(\theta/2)$	14.0
$p^{1/2}V^{4/3}B_T\sin^6(\theta/2)$	12.5
$P^{1/2}VB_T\sin^6(\theta/2)$	12.1
VB_s	8.91

$\sin^6(\theta/2)$ or $\sin^4(\theta/2)$?

Where $\sin^4(\theta/2)$ did appear from?

Kan and Lee (1978) model

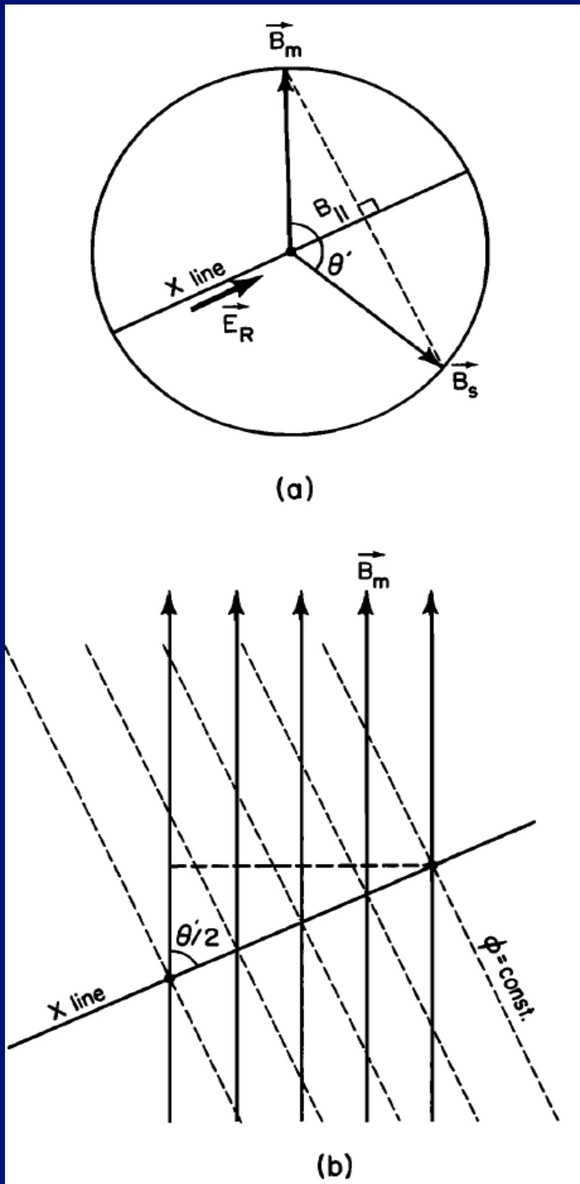

ig. 1. A schematic illustration of the field

$$E_R = V_s B_s \sin\left(\frac{\theta}{2}\right)$$

Reconnection Electric field for two magnetic fields of equal magnitudes: Sonnerup (1974) Russell and Atkinson (1973)

Kan and Lee stated that only perpendicular component of the electric field contributes to the potential across the polar

$$\Phi = \int E_{R\perp} dl_\perp = \int V_s B_s \sin^2\left(\frac{\theta}{2}\right) dl \sin\left(\frac{\theta}{2}\right)$$

$$\Phi = V_s B_s \sin^3\left(\frac{\theta}{2}\right) l_0$$

Finally Kan and Lee argued that power delivered by solar wind dynamo is proportional to potential square divided effective system resistance:

$$P = \frac{\Phi^2}{R} = V_s^2 B_s^2 \sin^6\left(\frac{\theta}{2}\right) l_0^2$$

ENERGY COUPLING FUNCTION AND SOLAR WIND–MAGNETOSPHERE DYNAMO

J.R. Kan and L.C. Lee

The potential difference Φ_m across the polar cap is due to the perpendicular component of the reconnection electric field, i.e., $E_R \sin \theta/2$ as shown in Figure 1(b). This geometrical factor has been overlooked in the previous studies of component reconnection. Thus the polar cap potential Φ_m can be written as

$$\Phi_m = V_s B_s \sin^2 (\theta/2) \ell_o \qquad (3)$$

where ℓ_o is the effective length of the X line.

The power delivered by the solar wind dynamo is given by

$$P = \phi_m^2/R = V^2 B^2 \sin^4 (\theta/2) \ell_o{}^2/R$$

$$= (V/R) \ \varepsilon (t) \qquad (5)$$